Article

Neuron

Motivation, Perception, and Chance Converge to Make a Binary Decision

Graphical Abstract

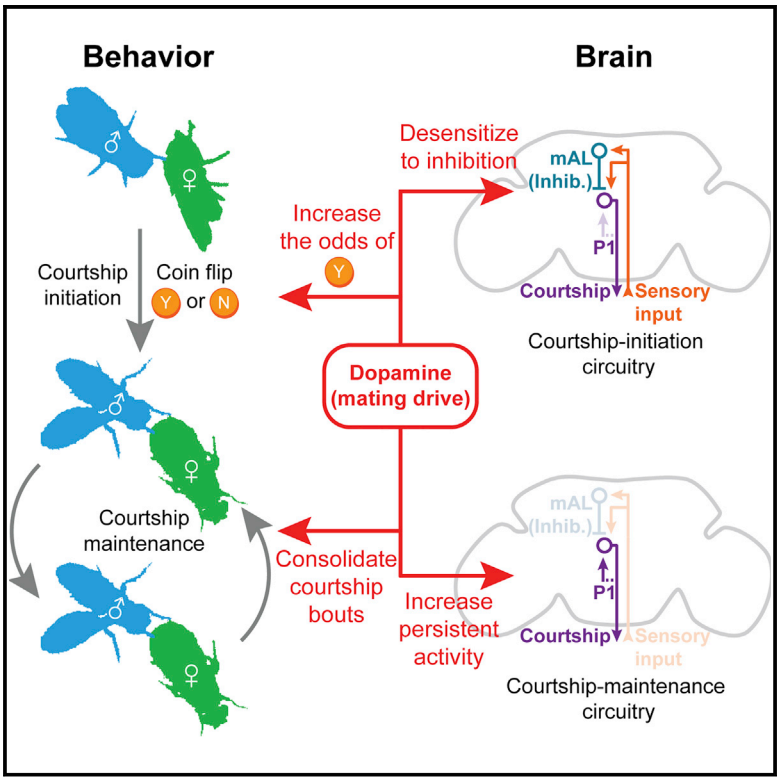

Highlights

- A coin-flip model describes the probability of courtship after contact with a female
- A dopaminergic signal sets courtship probability by desensitizing P1 to inhibition
- Dopamine sustains courtship by promoting recurrent P1 stimulation
- Receptor diversity allows motivational tuning of multiple circuit properties

Authors

Stephen X. Zhang, Lauren E. Miner, Christine L. Boutros, Dragana Rogulja, Michael A. Crickmore

Correspondence

dragana_rogulja@hms.harvard.edu (D.R.), michael.crickmore@childrens.harvard.edu (M.A.C.)

In Brief

Zhang et al. show that a dopaminergic signal motivates *Drosophila* courtship by adjusting circuit parameters to 1) increase the probability that a sensory stimulus will initiate behavior and 2) sustain behavior by decreasing the probability of termination.

Zhang et al., 2018, Neuron *99*, 1–13
July 25, 2018
https://doi.org/10.1016/j.neuron.2018.06.014

CellPress

Please cite this article in press as: Zhang et al., Motivation, Perception, and Chance Converge to Make a Binary Decision, Neuron (2018), https://doi.org/10.1016/j.neuron.2018.06.014

Neuron
Article

CellPress

Motivation, Perception, and Chance Converge to Make a Binary Decision

Stephen X. Zhang,[1] Lauren E. Miner,[2] Christine L. Boutros,[2] Dragana Rogulja,[1,*] and Michael A. Crickmore[2,3,*]
[1]Department of Neurobiology, Harvard Medical School, Boston, MA 02115, USA
[2]FM Kirby Neurobiology Center, Boston Children's Hospital, Harvard Medical School, Boston, MA 02115, USA
[3]Lead Contact
*Correspondence: dragana_rogulja@hms.harvard.edu (D.R.), michael.crickmore@childrens.harvard.edu (M.A.C.)
https://doi.org/10.1016/j.neuron.2018.06.014

SUMMARY

We reveal a central role for chance neuronal events in the decision of a male fly to court, which can be modeled as a coin flip with odds set by motivational state. The decision is prompted by a tap of a female with the male's pheromone-receptor-containing foreleg. Each tap evokes competing excitation and inhibition onto P1 courtship command neurons. A motivating dopamine signal desensitizes P1 to the inhibition, increasing the fraction of taps that successfully initiate courtship. Once courtship has begun, the same dopamine tone potentiates recurrent excitation of P1, maintaining the courtship of highly motivated males for minutes and buffering against termination. Receptor diversity within P1 creates separate channels for tuning the propensities to initiate and sustain courtship toward appropriate targets. These findings establish a powerful invertebrate system for cue-triggered binary decisions and demonstrate that noise can be exploited by motivational systems to make behaviors scalable and flexible.

INTRODUCTION

Motivational states and external conditions strongly influence behavior (Halliday, 1983; Toates, 1986). But would the same animal, in the same state, presented with the same circumstance always make the same decision? If not, this variability presumably emerges from noise and hidden network variables as information propagates through the nervous system (Faisal et al., 2008; Renart and Machens, 2014). Though often considered a flaw, noise—or network variability—has been shown to be useful for improving signal detection and implementing ideal strategies in adversarial situations and has also been proposed to promote exploration (Faisal et al., 2008; Ölveczky et al., 2005; Tervo et al., 2014). Here, we show how noise is used by motivational circuitry to effect probabilistic changes in behavior.

In a growing number of systems, neurons that alter behavioral probabilities have been localized to small, spatially restricted, and genetically targetable populations. In the best-studied example, stimulating the ~800 AgRP neurons of the arcuate nucleus in the mouse hypothalamus induces seemingly all aspects of hunger: eating available food, foraging, and performing arbitrary tasks previously associated with food rewards (Aponte et al., 2011; Betley et al., 2015; Chen et al., 2016; Krashes et al., 2011; Livneh et al., 2017). Subpopulations of AgRP neurons that target single brain regions coordinately regulate the latency to eat and the quantity of food consumed (Betley et al., 2013). A similar connection between the probabilities of initiation and maintenance of behavior is seen during stimulation of the galanin neurons of the medial preoptic area of the hypothalamus, which induce the initiation of parental behavior and also extend the duration of parenting bouts (Wu et al., 2014). In these examples, the sensory inputs (food, offspring) and motor outputs (feeding, parenting) are the same across behavioral selection and duration, suggesting shared circuitry—but control over the binary decision to initiate the behavior and the scalar determination of its duration likely require different regulatory mechanisms.

We examined the links between behavioral selection, persistence, and chance using *Drosophila* courtship, which we recently found to be under motivational control (Zhang et al., 2016). Upon encountering a potential mate, a male must first choose whether or not to initiate courtship. Then, at every subsequent moment until the initiation of copulation, he must decide whether or not to persist in the courtship that has so far been unsuccessful. Males with high mating drive sustain courtship for minutes, whereas courtship by satiated males, when it occurs, is frequently abandoned. The male's motivation to court hinges on the dopaminergic activity of a few neurons that project to a brain region called the anterior of superior medial protocerebrum (SMPa) (Zhang et al., 2016). In naive males, dopaminergic activity is high, and the presentation of a virgin female almost always leads to courtship. After a few matings, dopaminergic activity decreases and these satiated males mostly abstain from courtship. The dopaminergic mating drive signal is received by a group of ~20 command neurons, called P1, which are stimulated by sensory information from the female and orchestrate the many behavioral programs that constitute courtship (Clowney et al., 2015; Kallman et al., 2015; Kohatsu and Yamamoto, 2015; Kohatsu et al., 2011; Pan et al., 2012; von Philipsborn et al., 2011; Zhang et al., 2016). We find that the propensity for initiation and termination are both instructed by the same dopaminergic signal to P1 but result from separate cellular mechanisms. In analogy to combustion: dopamine is the fuel that increases the odds that a spark will kindle a fire, and that determines how long it burns.

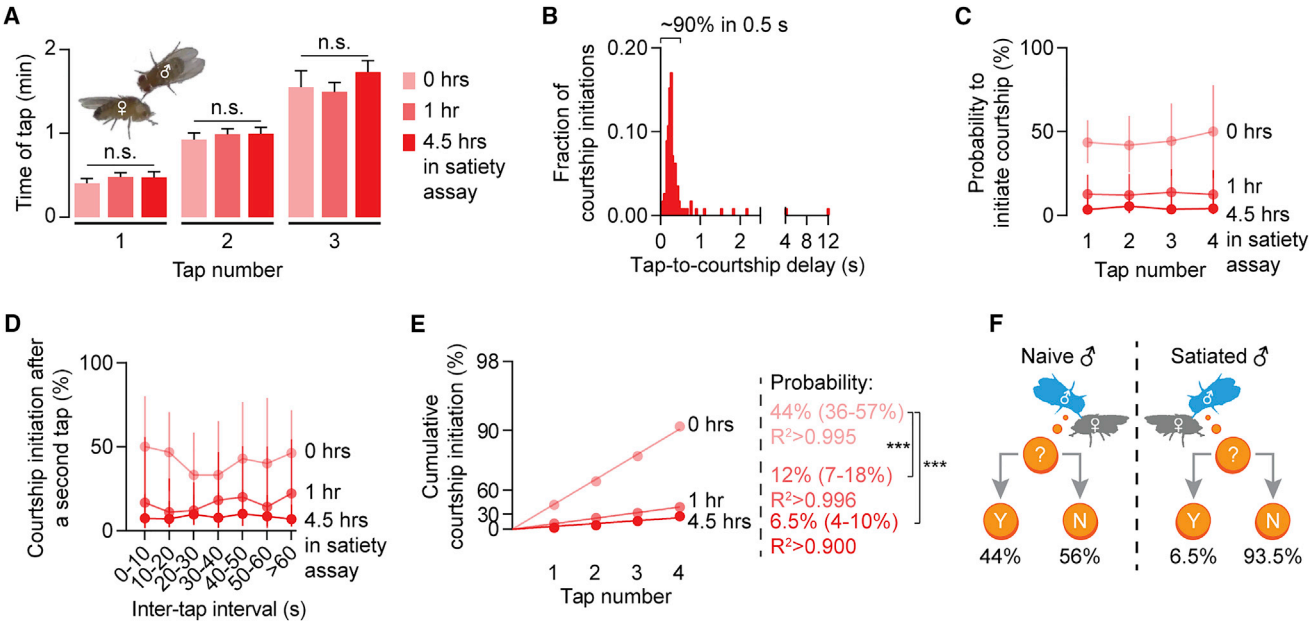

Figure 1. A Coin-Flip Model Describes Courtship Initiation Probability

(A) The tapping frequency over the first several minutes in a courtship assay is consistent from tap to tap and does not change with satiety state (see STAR Methods) (one-way ANOVA†, n = 47–57 males).

(B) Courtship is always preceded by a tap (n = 112 initiations). See Videos S1, S2, and S3.

(C and D) The per-tap probability to initiate courtship scales with satiety state but is consistent from tap to tap (C) and is independent of the inter-tap interval (D) (mean ± 95% CI, n = 47–57 males).

(E) For each satiety state, the cumulative courtship initiation probability curve linearizes on a modified log-scaled y axis suitable for coin-flip models (see STAR Methods). The courtship probabilities are calculated from the slopes of the linear fits (95% CI are in parentheses; bootstrap, n = 47–57 males; see details for bootstrapping in STAR Methods).

(F) Motivation sets the probability that a tap will trigger courtship.

†In all figures, *p < 0.05, **p < 0.01, ***p < 0.001; n.s., not significant for all statistical tests. See Table S1 for all estimated courtship probabilities and Table S2 for genotypes and the numbers of animals for each experiment.

RESULTS

A Coin-Flip Model of Courtship Initiation

For the first several minutes after being placed in a 1-cm courtship chamber, naive male flies tapped virgin females with their pheromone-receptor-bearing forelegs once every 30 s (Figures 1A and S1A and Videos S1 and S2) (Thistle et al., 2012). Each tap led to courtship ~44% of the time, almost always within 500 ms of the tap (Figure 1B), and regardless of whether it was the 1st, 2nd, 3rd, or 4th tap (Figure 1C), or of the interval between taps (Figure 1D). While certain mutations (Billeter et al., 2009; Manoli and Baker, 2004) and conditions (Agrawal et al., 2014; Fan et al., 2013) may obviate the requirement for a tap, in our experimental setup (see STAR Methods) we have yet to observe courtship from a wild-type or control male (2,147 in this paper) that was not preceded by a tap (see also Kohatsu et al., 2011; Rendel, 1945; Spieth, 1952, 1974). We present courtship probabilities as linear natural log plots of (1 – [cumulative probability]) against tap number (e.g., Figure 1E), where the fitted slope indicates courtship probability and the R^2 value reflects the consistency of tap-to-tap probabilities (see Table S1 for all courtship probabilities with 95% confidence intervals; see Figures S1B–S1D for p value distributions of R^2 values compared to a coin-flip model and a permutation test). We typically find R^2 values greater than nearly all permutated possibilities, indicative of the remarkable consistency in the probability of each tap to trigger courtship (see Figure S1B for an example; see Figure S1D for all comparisons). These results show that the probability of courtship initiation can be well described by a simple coin-flip model with two variables: the bias of the coin (probability of courtship initiation after a tap) and how often it is flipped (tapping frequency).

To assess the effect of sensory input on courtship probability, we presented the male with a mated female, who is unlikely to allow copulation and is therefore a lower-quality stimulus (Tompkins and Hall, 1981). While the frequency of tapping did not change (Figure S1E), the tap-induced courtship probability dropped to ~7%, again consistent from tap to tap (Figure S1F). The male therefore decreases courtship toward a less appropriate target by scaling down the tap-driven initiation probability.

To assess the effect of motivational state on the courtship decision, we tested males that had spent various amounts of time in the satiety assay: a single male paired with ~20 virgin females and allowed to mate *ad libitum* (Zhang et al., 2016). After several matings, satiated males exhibited a tapping frequency that was identical to that of naive males (Figure 1A), but the probability that a tap led to courtship gradually declined as satiety increased, sinking to 6.5% after 4.5 hr in the satiety assay

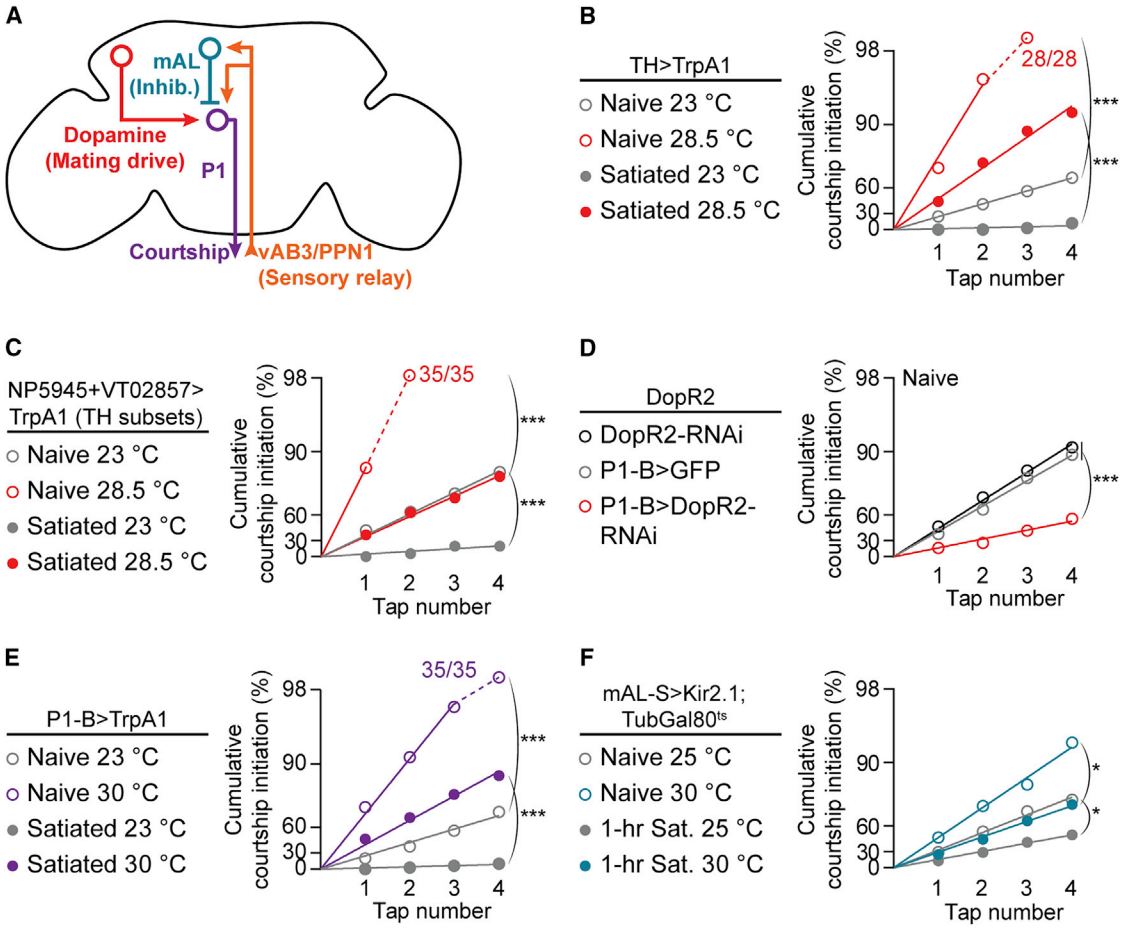

Figure 2. Dopamine Sets Courtship Probability by Desensitizing P1 to Inhibition

(A) Motivational and sensory inputs to P1 neurons.

(B–D) Courtship probability is increased by stimulating dopaminergic neurons (B) that project to the SMPa (C) and is decreased by knocking down DopR2 in P1-B neurons (D) (bootstrap, B: n = 26–31 males, C: n = 29–35, D: n = 23–33). Off-y-axis circles indicate 100% courtship initiation. See Figure S2A for no-Gal4 controls for (B) and (C). See Figures S4B and S4C for stimulating either dopaminergic population alone.

(E and F) Stimulating P1-B neurons (E) or conditionally silencing mAL neurons (F) increases courtship probability (bootstrap, E: n = 27–35 males, F: n = 28–35). Conditional silencing was achieved by raising flies at 23°C until eclosion and then shifting half of them to 30°C for 3 days before testing. See Figures S2B and S2C for no-Gal4 controls.

(Figures 1C, 1D, and S1A and Video S3). Though courtship initiation probability was profoundly influenced by satiety state, it was again remarkably consistent from tap to tap within a given treatment (Figures 1C and 1D). These results align well with traditionally used courtship metrics such as courtship latency and courtship index (Figures S1G and S1H). Together, they demonstrate that stimulus quality and motivational state combine to produce a fixed probability of courtship elicited by each tap (Figure 1F).

Dopamine-to-P1 Signaling Determines Tap-Induced Courtship Probability

Dopaminergic activity in the SMPa is a functional neuronal correlate of mating drive (Zhang et al., 2016). This dopamine signal is received by P1 courtship command neurons that also integrate sensory cues from tapping (Figure 2A) (Clowney et al., 2015; Kallman et al., 2015; Kohatsu and Yamamoto, 2015; Kohatsu et al., 2011; Zhang et al., 2016). To examine the effect of dopamine tone on the probability that a tap will induce courtship, we thermogenetically stimulated either all dopaminergic neurons or just the subsets that have been shown to promote mating drive (Zhang et al., 2016). Dopaminergic stimulation dramatically increased per-tap probability (Figures 2B, 2C, S2A, S3A–S3D, S4B, and S4C; see Figures S3E–S3H for silencing experiments) but did not affect tapping frequency (Figure S4A), and initiation probabilities were again well described by the coin-flip model. Note that dopaminergic stimulation increased courtship probability not only in satiated males, but also in naive males. We see this effect in all of our manipulations that elevate mating drive and believe it reflects a general property of motivation: the range under normal conditions is only a fraction of that which the circuitry is capable of producing, as seen following narcotic use or under pathological conditions (Wise and Rompre, 1989).

P1 command neurons drive entry into the courtship state when activated (Anderson, 2016; Kohatsu and Yamamoto, 2015; Pan et al., 2012; von Philipsborn et al., 2011; Yamamoto and Koganezawa, 2013; Zhang et al., 2016). The motivating dopamine signal is received at P1 by the DopR2 receptor, and a satiety-like state is induced by knocking down the receptor from P1 (Zhang et al., 2016). Accordingly, we find a decreased per-tap courtship probability when DopR2 is knocked down in P1 neurons (Figure 2D), and that thermogenetic stimulation of P1 dramatically increases tap-induced initiation probability (Figures 2E and S2B). Note that more intense or prolonged P1 stimulation can lead to courtship that does not require a tap, but under our conditions a tap always preceded courtship. These results are consistent with the idea that dopamine sets courtship probabilities by scaling the likelihood that a tap will drive super-threshold P1 activation.

Dopamine Tone Adjusts the Sensitivity of P1 Neurons to Inhibition

In addition to the motivating dopamine signal, P1 neurons also integrate sensory inputs: each tap evokes parallel excitation (via vAB3 and PPN1 neurons) and inhibition (via mAL neurons) onto P1 (Figure 2A) (Clowney et al., 2015; Kallman et al., 2015; Kohatsu and Yamamoto, 2015; Kohatsu et al., 2011). While past studies focused on shifting excitation/inhibition in response to courtship targets of varying quality, we asked whether dopamine might tune these competing inputs to scale tap-induced P1 activation to motivational state, thereby adjusting the threshold for courtship initiation. Thermogenetic stimulation of excitatory inputs to P1 (vAB3 or PPN1) did not increase courtship behavior from satiated males (Figures S5A and S5B), but silencing the inhibitory mAL neurons, which have been shown to prevent male-male courtship (Kallman et al., 2015), strongly promoted courtship toward females (Figures 2F and S2C). While the impact of silencing mAL was robust after 1 hr in the satiety assay, it was weaker following a standard 4.5-hr satiety assay (data not shown). Data we present below argue that the incompleteness of this effect is due to the existence of other inhibitory neurons not labeled by the mAL-S Gal4 line (R43D01, named after the Scott lab where it was first characterized; Kallman et al., 2015). These other inhibitory inputs likely include neurons that mediate the courtship-suppressing effects of volatile pheromones (Billeter et al., 2009). For consistency throughout the manuscript, we examine behavior after 1-hr satiety assays except when attempting to acutely revert satiety post hoc with thermogenetic stimulation, which we test following completion of 4.5-hr assays. Note that silencing mAL neurons also increases courtship probability in naive males (Figures 2F and S2C), indicating that mAL neurons moderate courtship behavior, even when highly motivated males contact virgin females.

One possible mechanism for decreasing courtship probability in satiated males would be to increase the inhibitory output of mAL neurons in response to a tap. However, we considered this mechanism unlikely due to the position of mAL in courtship circuitry (Figure 2A): the dopamine mating drive signal is received, apparently exclusively, through the DopR2 receptors of P1 courtship command neurons (Zhang et al., 2016), which lie downstream of mAL (Clowney et al., 2015; Kallman et al., 2015). Consistent with this supposition, vAB3-to-mAL transmission did not change with satiety state (Figures 3A and S5C). We therefore considered the possibility that dopamine modulates the sensitivity of P1 neurons to GABAergic input from mAL.

We found that the net excitation of P1 by vAB3 seen in naive males was absent from the brains of satiated males (Figures 3B and S5D), in accordance with the inability of vAB3 stimulation to revert satiety (Figure S5A; see Figure S5B for similar results with PPN1). Excitation of P1 by vAB3 is restored in satiated males by the $GABA_A$ blocker picrotoxin (PTX; Figure 3B), suggesting that an increase in the sensitivity of P1 to GABA may underlie the inability of a tap to drive courtship in satiated males. Consistent with this idea, the voltage sensor ASAP1 (St-Pierre et al., 2014) revealed an increased hyperpolarization of P1 neurons in response to mAL stimulation in satiated males (Figure 3C). This increased sensitivity to inhibitory input is not associated with any obvious change in mAL-P1 connectivity (Figure S5E) and is reverted by application of dopamine (Figure 3C), providing evidence that dopamine desensitizes P1 neurons to GABAergic inhibition from mAL. Desensitization to inhibition evoked by a sensory stimulus may be a widespread mechanism for motivational control, as it allows drive signals to promote behavior while retaining the requirement for strong excitatory input (Halliday, 1983; Zhang et al., 2016).

Together, these results suggest that the local dopamine tone sets a threshold that the sensory stimulus and chance events must cross to drive courtship (Figure 3D). This is accomplished by modulating the responsiveness of P1 neurons to inhibition triggered by a tap of even a high-quality stimulus. In a satiated male, the full force of inhibition is perceived by P1, so only the small fraction of taps that, by chance, generate an unusually strong excitation-to-inhibition ratio will be sufficient to drive courtship. As dopamine tone increases with time away from females, P1 becomes less and less sensitive to inhibitory input, allowing an increasing fraction of upstream circuit outcomes to produce super-threshold P1 activation.

A Specialized $GABA_A$ Subunit Mediates Satiety in P1 Neurons

If dopamine desensitizes P1 neurons to inhibition, how is the selection against low-quality targets maintained under high drive conditions? It has been shown (Kallman et al., 2015), and we confirm (Figures 4A and S5F), that the $GABA_A$ receptor Rdl is required in P1 neurons to prevent males from courting other males. This appears to be a sensory (i.e., not motivational) phenotype because we found no impact of Rdl knockdown on female-directed courtship (Figures 4B and S5G). To identify the GABA receptor that receives the satiety-related inhibitory input from mAL, we screened RNAi lines targeting other predicted GABA receptors. We identified pHCl, a chloride channel that has homology with $GABA_A$ and GlyR receptors but does not itself bind GABA and therefore likely constitutes part of a heteromeric $GABA_A$ receptor (Schnizler et al., 2005). Knocking down pHCl in P1 neurons reduced mAL-induced inhibition at P1 (Figure 4C) and dramatically increased courtship probability toward virgin females (Figure 4D), without causing male-directed courtship (Figure 4E). Normal courtship probabilities are restored to DopR2 mutants by knocking down pHCl in P1 neurons (Figure 4F), supporting the idea that dopamine promotes mating

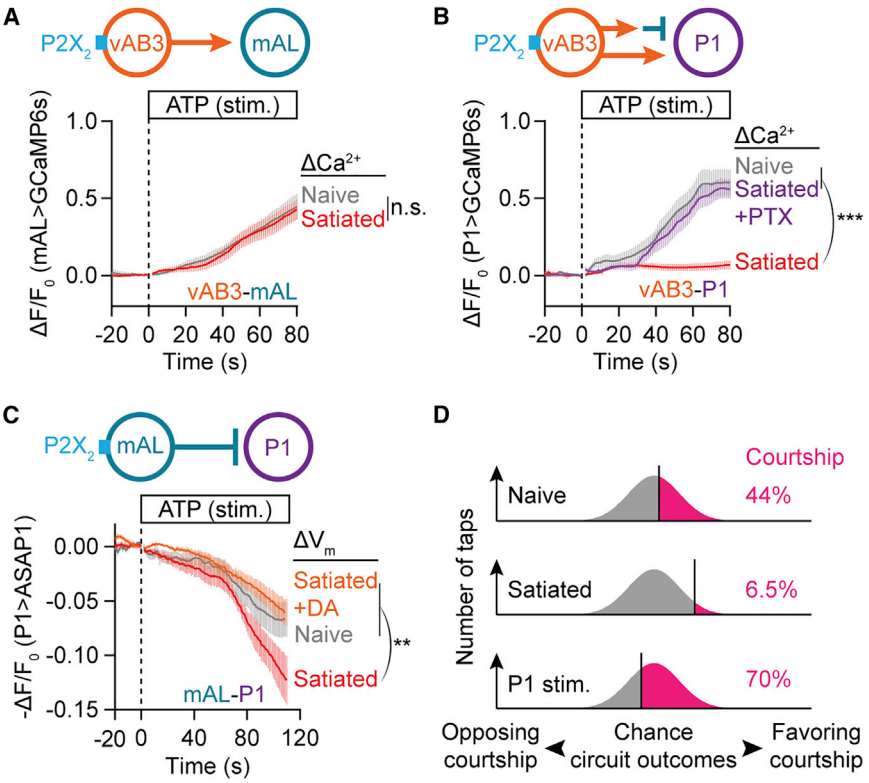

Figure 3. Dopamine Desensitizes P1 to Inhibition

(A) $P2X_2$ stimulation (Lima and Miesenböck, 2005) of vAB3 axons evokes the same calcium response in mAL neurons from naive and 4.5-hr-satiated males (t test of max $\Delta F/F_0$, mean ± SEM, n = 12–13 brains). See Figure S5C for subsequent KCl stimulation, which shows these neurons to be healthy.

(B) $P2X_2$ stimulation of vAB3 axons evokes a strong calcium response in P1-B neurons only in brains dissected from naive (gray) but not 4.5-hr satiated males (red). A strong calcium response is recovered in satiated brains by pre-applying 100 μM $GABA_A$ blocker picrotoxin for 10 min before ATP stimulation (purple) (one-way ANOVA of max $\Delta F/F_0$, mean ± SEM, n = 14–15 brains). See Figure S5D for subsequent KCl stimulation.

(C) $P2X_2$ stimulation of mAL neurons hyperpolarizes P1 neurons, as indicated by an increase in the fluorescence (decrease in $-\Delta F/F_0$) of the ASAP1 voltage sensor. This hyperpolarization is more pronounced in brains dissected from 4.5-hr satiated males (red) than from naive males (gray). The increased sensitivity to mAL stimulation in satiated brains is reverted by pre-applying 100 μM dopamine for 10 min before ATP stimulation (orange) (one-way ANOVA of min $-\Delta F/F_0$, mean ± SEM, n = 8–9 brains). In this and subsequent voltage-imaging plots, fluorescence changes are plotted on a $-\Delta F/F_0$ scale to correct for the inverse relation between membrane voltage and sensor fluorescence (St-Pierre et al., 2014).

(D) Motivation and P1 stimulation shift the fraction of taps that generate excitation/inhibition ratios sufficient to trigger courtship.

drive by selectively desensitizing P1 neurons to GABA that is received by pHCl complexes. The sensory discrimination and motivational impacts of mAL activity therefore act through distinct GABA receptors in P1 neurons. This splitting of the GABAergic mAL signal into drive-specific (via pHCl) and target-specific (via Rdl) inhibitory channels prevents courtship of inappropriate targets, even when mating drive is high (Figure 4G).

A Memoryless Coin-Flip Mechanism Improves Target Selection

At the core of the coin-flip model is the idea that male flies make independent decisions from tap to tap. Alternatively, the male could accumulate evidence for or against courtship after each tap, until the compiled evidence (both sensory- and drive-related) reaches the threshold for courtship. Arguing against an evidence-accumulation model is the fact that the per-tap courtship probability does not depend on inter-tap interval (Figure 1D), meaning that if evidence is retained after a tap, it does not substantially decay over 60 s. Nevertheless, our tapping data could also be well described by a computational algorithm designed for evidence accumulation (Figure S6; see STAR Methods) (Drugowitsch et al., 2012). We therefore designed a more stringent test of the coin-flip model for target selection.

Evidence accumulation is beneficial under many circumstances but could lead to errors if the world imperceptibly changes—in our case, if the female changes. For example, evidence collected from a tap of a mated female might reduce the courtship probability generated by a subsequent tap of a virgin female. Intuitively then, the coin-flip model does outperform our evidence-accumulation model for selection of the virgin when a mated female is also present (Figure 5). To see which model best fits the male's behavior, we placed a naive male together with one mated and one virgin female and found that the fraction of times the male courted the virgin was consistent with the coin-flip model (Figure 5). These results support our conclusion that the male fly makes independent decisions from tap to tap. Independent sampling can be a beneficial strategy when the sensory source is ambiguous; these results show that this strategy is used by the male's courtship circuitry to ensure that both the female and his own drive state are appropriate before initiating courtship.

A Shared Mechanism for Permitting Initiation and Preventing Termination of Courtship

Not all courtship will lead to copulation, so, after initiation, a courting male must constantly judge whether heretofore unfruitful courtship is worth sustaining. For naive, highly motivated males, unsuccessful courtship is usually maintained for several minutes. With increasing satiety, however, the average courtship bout length progressively decreases (Figure 6A). We noticed that roughly half of all courtship terminations were immediately

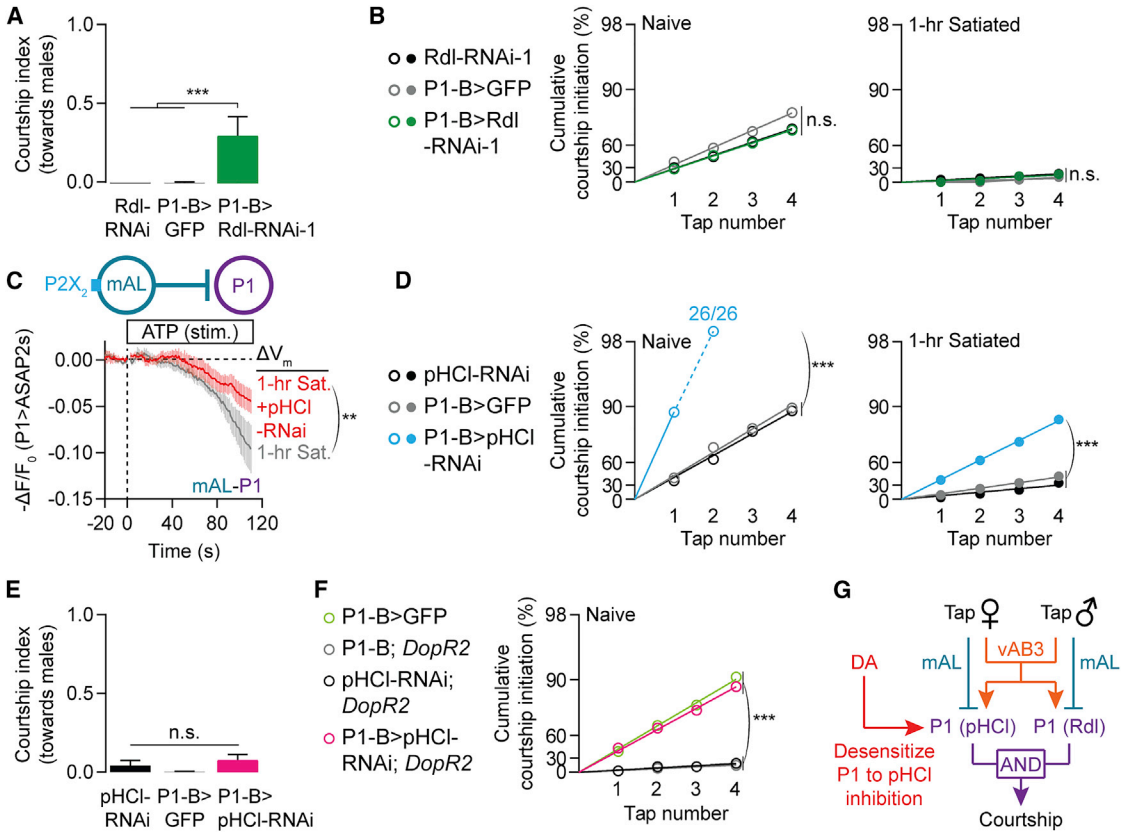

Figure 4. Dopamine Tunes P1's Response to Inhibition from Female Contact

(A and B) RNAi knockdown of Rdl in P1 neurons increases courtship of male (A) but not female (B) targets (A: mean ± SEM, one-way ANOVA, n = 13–16 males; B: bootstrap, left: n = 28–30, right: n = 28–33). See Figures S5F and S5G for similar results using a second, independent Rdl-RNAi line.

(C) pHCl knockdown in P1 neurons decreases the inhibitory effect of mAL in 1-hr satiated males, as indicated by a smaller deflection from baseline reported by the ASAP2s voltage sensor (t test of min $-\Delta F/F_0$, n = 8 males each) (Chamberland et al., 2017).

(D and E) Knocking down pHCl in P1 neurons increases courtship of female (D) but not male (E) targets (D: bootstrap, left: n = 26–29 males, right: n = 24–30; E: mean ± SEM, one-way ANOVA, n = 11–30).

(F) pHCl knockdown in P1 neurons rescues the low courtship probability phenotype in naive males lacking the DopR2 receptor (bootstrap, n = 30–42 males).

(G) pHCl and Rdl convey motivation-dependent and sensory-dependent inhibition to P1 neurons, respectively.

preceded by contact with the female (Figures 6B–6D, S1A, S7A, and S7B and Video S4), much more often than would be expected by chance (Figure 6D). When we stimulated dopaminergic or P1 neurons in satiated males, we saw strong reductions in both contact-related (tap-induced) and spontaneous terminations (Figures 6E, S2D, S2E, S3I–S3L, and S4D–S4G). When the connection between dopamine and P1 was severed by knocking down the DopR2 receptor in P1 neurons, naive males showed levels of tap-induced and spontaneous terminations that were similar to those seen in satiated males (Figure 6F). None of these manipulations changed the tapping frequency during courtship (Figures S7C–S7K). The same dopamine-to-P1 signal that instructs the probability of initiating courtship therefore also dictates the moment-to-moment probability of termination, coordinating two central facets of motivation: behavioral selection and persistence.

Given its role in suppressing courtship initiation, we considered mAL a likely candidate for carrying a tap-induced termination signal. Consistent with this prediction, silencing mAL neurons resulted in a near complete loss of tap-induced terminations (Figures 6G and S2F), and brief optogenetic stimulation of mAL during courtship induced termination (Figure 6H). Brief pulses of optogenetic inhibition delivered to P1 via the green-light gated chloride channel GtACR1 (Mohammad et al., 2017) were also sufficient to disrupt ongoing courtship (Figures 6I and S5H). P1 activity is therefore required to maintain the courtship state and can be inhibited by mAL during ongoing courtship. The mechanism through which the GABAergic termination signal is transduced at P1 appears to be the same as is used for suppression of courtship initiation, requiring the pHCl receptor, but not the Rdl receptor (Figures 6J, S5I, and S5J). These results show that dopamine prevents tap-induced termination in the same way it promotes courtship initiation: by decreasing the sensitivity of P1 neurons to GABAergic inhibition from mAL (Figure 6K). While a tap from a highly motivated male delivers strong courtship-inducing excitation to P1 (Clowney et al., 2015), in satiated males increased sensitivity of P1 to GABA causes the same sensory stimulus to trigger essentially the opposite result: abandonment of courtship.

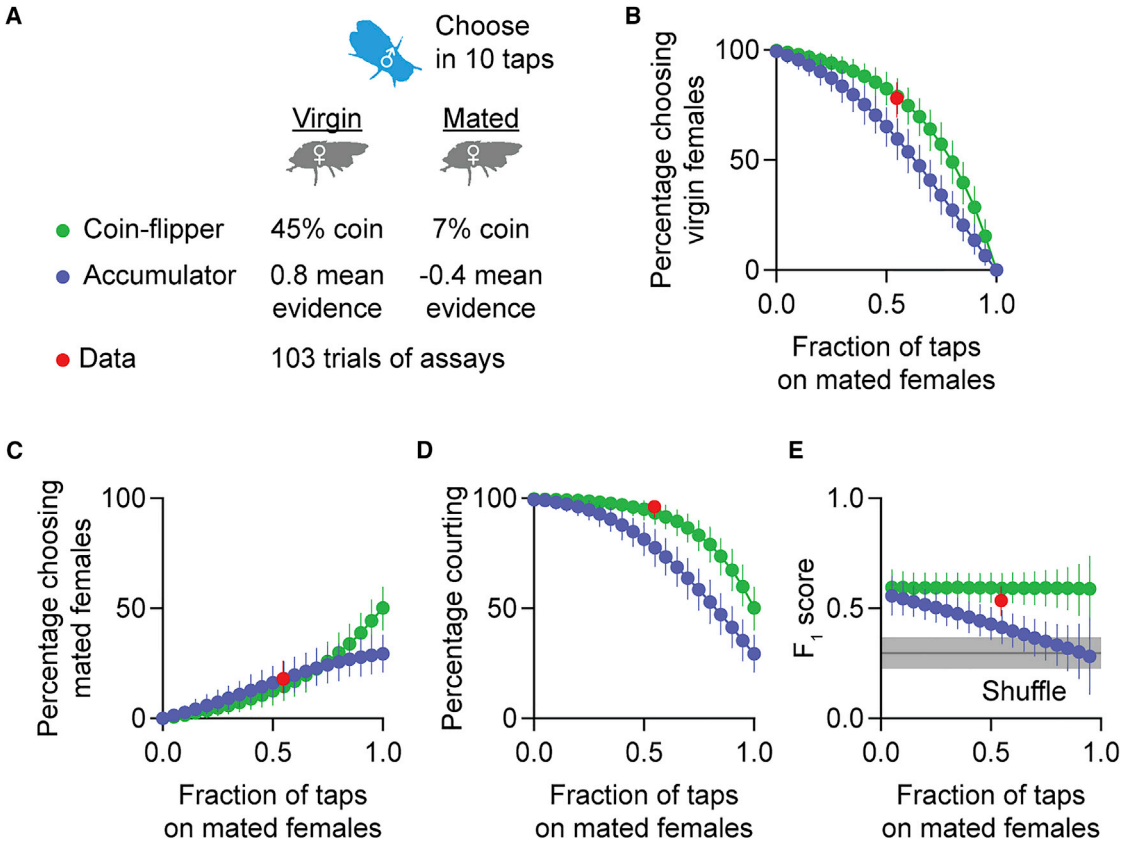

Figure 5. Accumulation and Coin-Flip Models for Courtship Target Selection

(A) Parameters for simulating a coin-flipper or an accumulator male fly in the courtship-choice assay. See Figure S6 for the parameter selection.

(B–D) Simulations predict that coin-flippers court virgin females (B) more often than evidence accumulators. The two models predict similar levels of courtship toward mated females (C), but coin-flippers court more overall (D). Experimental data (red) are similar to predictions from the coin-flipper simulation (n = 103 males, all results are shown as mean ± 95% CI; see STAR Methods for simulation details).

(E) Both coin-flipper-modeled males and actual males court virgin females more selectively (i.e., have higher F_1 scores) than accumulators (n = 103 males, all results are shown as mean ± 95% CI; gray shade shows mean ± 95% CI; F_1 scores of shuffled experimental data; see STAR Methods for simulation details).

Different Cholinergic Receptors Promote the Initiation and Maintenance of Courtship

mAL-induced inhibition of P1 cannot explain the ~50% of terminations that do not occur within 1 s after a tap (Figure S1A and Video S5): neither mAL silencing nor pHCl or Rdl knockdown in P1 neurons decreased the frequency of these spontaneous terminations (Figures 6G, 6J, S5I, and S5J). While acute optogenetic stimulation of dopamine neurons immediately restores a high courtship initiation probability to satiated males, maintenance of courtship requires a longer stimulation period (Figures 7A–7C). To search for the mechanisms that determine the rates of spontaneous termination downstream of prolonged dopamine signaling, we performed a screen targeting G proteins that might transduce the DopR2 signal. We found that knocking down $G\alpha_s$ in P1 neurons using two independent RNAi lines caused frequent spontaneous terminations without affecting courtship initiation or tap-induced termination (Figures 7D, 7E, S8A, and S8B). These results suggest that dopaminergic control of courtship drive bifurcates downstream of DopR2: a $G\alpha_s$-insensitive pathway desensitizes P1 to tap-related suppression, while a $G\alpha_s$-sensitive pathway sustains courtship in the inter-tap interval.

To begin to understand how the DopR2-to-$G\alpha_s$ signal in P1 neurons maintains courtship between taps, we screened through all known and predicted receptors for acetylcholine, the primary excitatory neurotransmitter in *Drosophila*. Knockdown of the nicotinic acetylcholine receptor nAChRα3 (nAChRα3 in mammals) in the P1 neurons of naive males resulted in decreased courtship initiation probability (Figures 7F and S8C) and frequent tap-induced termination (Figures 7G and S8D), but the spontaneous termination rate remained unaffected (Figures 7G and S8D). In contrast, knockdown of nAChRα6 (nAChRα7 in mammals) in P1 neurons did not alter tap-induced initiation or termination probabilities but caused a substantial increase in spontaneous termination rate (Figures 7H, 7I, S8E, and S8F). Here again, neurotransmitter receptor diversity allows dopamine to tune specific properties of command neurons. In this instance, the two receptors control behavioral dynamics on vastly different timescales (~500 ms versus min), reflecting the rapid decision to initiate behavior in response to excitation

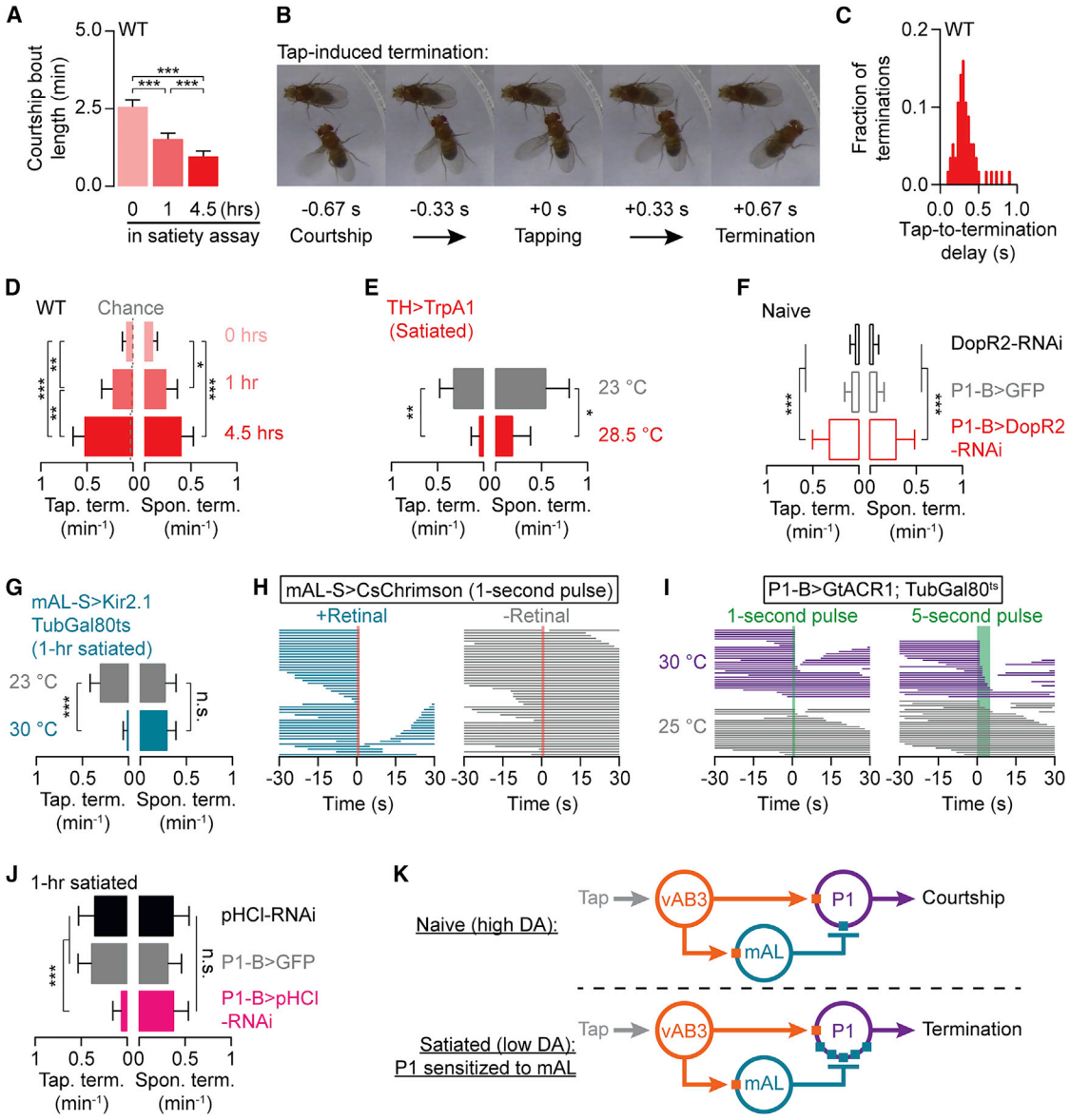

Figure 6. Dopamine Tone at P1 Determines the Duration of Courtship Bouts

(A) Courtship becomes increasingly fragmented with satiety (mean ± SEM, one-way ANOVA, n = 47–57 males).

(B) An example of a tap-induced termination (see STAR Methods for classification criteria; see Video S4 for a sample fly).

(C) When a tap terminates courtship, it typically does so with short (<0.5 s) latency (n = 56 courtship terminations).

(D) Both tap-induced (left) and spontaneous terminations (right) (see Video S5 for a sample fly) become more frequent with increasing satiety (mean ± 95% CI, Fisher's exact test‡, n = 47–57 males). Dashed lines in (D) indicate chance levels of tap-induced termination (see STAR Methods).

(E) Thermogenetic stimulation of dopaminergic neurons decreases both tap-induced and spontaneous termination in 4.5-hr-satiated males (mean ± 95% CI, Fisher's exact test, n = 26–31 males). See Figure S2D for no-Gal4 controls.

(F) RNAi knockdown of the DopR2 receptor in P1-B neurons increases both tap-induced and spontaneous terminations in naive males (mean ± 95% CI, Fisher's exact test, n = 23–33 males).

(G) Conditional silencing of mAL neurons prevents tap-induced, but not spontaneous, terminations in 1-hr-satiated males (mean ± 95% CI, Fisher's exact test, n = 28–35 males). See Figure S2F for no-Gal4 controls.

(H) Optogenetic stimulation of mAL neurons terminates ongoing courtship (left), only in the presence of the obligate chromophore retinal (right).

(I) Optogenetically silencing P1-B neurons during courtship mimics tap-induced terminations (purple). Light alone does not terminate courtship (gray; also see Figure S5H for the no-Gal4 control).

(J) Knocking down pHCl in P1-B neurons prevents tap-induced, but not spontaneous, terminations in 1-hr-satiated males (mean ± 95% CI, Fisher's exact test, n = 24–33 males).

(K) Motivation sets the probability of tap-induced termination by altering P1's sensitivity to mAL-derived inhibition.

‡In all figures, Fisher's exact tests are used with Bonferroni correction to adjust for multiple comparisons.

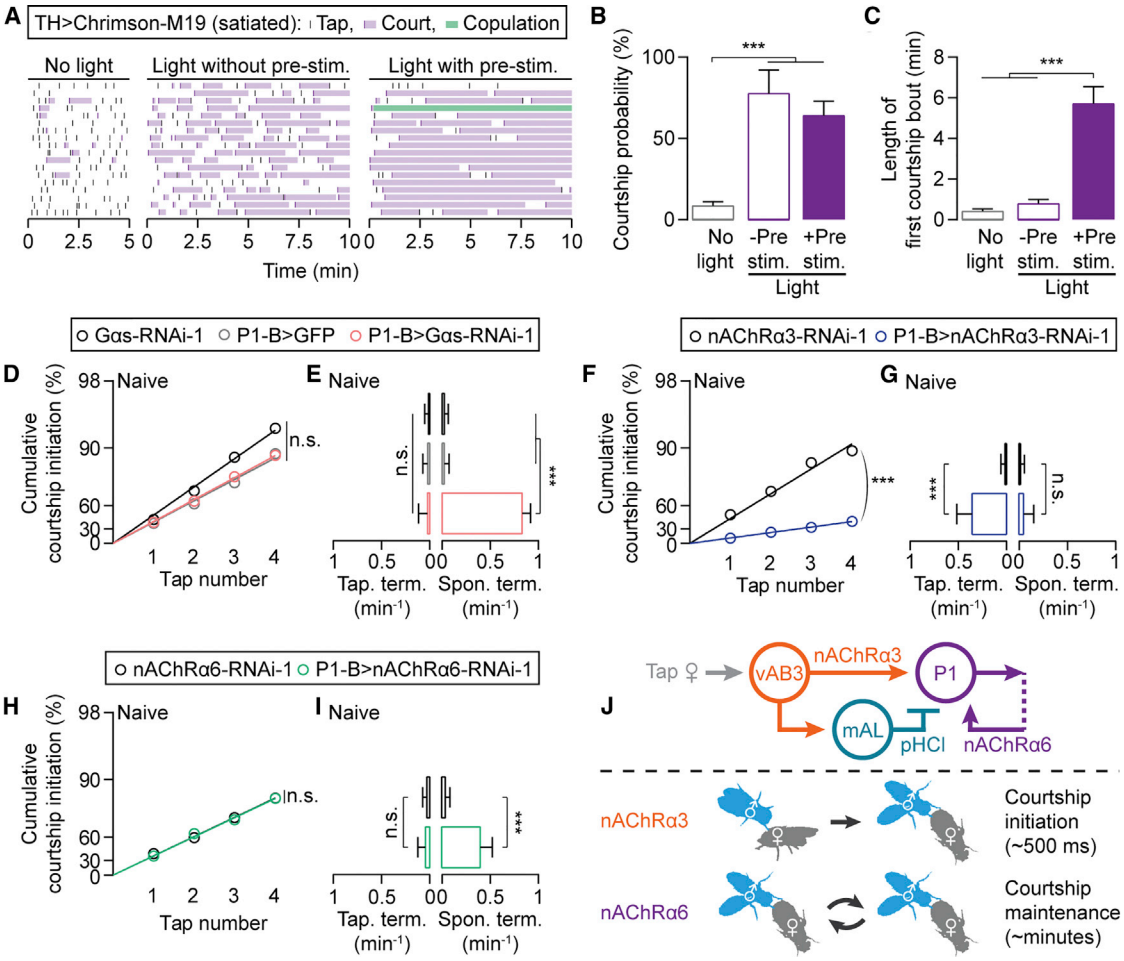

Figure 7. Separate Excitatory Channels at P1 for Initiation and Maintenance of the Courtship State

(A–C) Acute stimulation of dopaminergic neurons in satiated males immediately restores courtship-initiation probability (see A for ethogram and B for quantification), but prolonged stimulation is required for courtship maintenance (see A for ethogram and C for quantification) (B: mean ± 95% CI, bootstrap; C: mean ± SEM, one-way ANOVA; n = 18 males for each condition).

(D and E) RNAi knockdown of $G\alpha_s$ does not affect courtship initiation (D) or tap-induced termination (E) but increases spontaneous termination frequency (E) (D: bootstrap; E: mean ± 95% CI, Fisher's exact test; n = 25–32). See Figures S8A and S8B for similar results using a second, independent RNAi line.

(F–I) Knocking down nAChRα3 (F and G) or nAChRα6 (H and I) in P1 neurons selectively influences tap-dependent (F and G) and tap-independent (H and I) courtship transitions, respectively (F and H: bootstrap; G and I: mean ± 95% CI, Fisher's exact test; F and G: n = 28–34 males, H and I: n = 32–38). See Figures S8C–S8F for similar results using second, independent RNAi lines.

(J) Model: nAChRα3 mediates tap-evoked excitation from vAB3 to P1. nAChRα6 mediates recurrent excitation at the P1 locus, maintaining the courtship state.

via nAChRα3, and the long-term maintenance of P1 activity, presumably a consequence of recurrent stimulation of P1 that is received through nAChRα6 (Figure 7J).

Dopamine Promotes Sustained P1 Calcium Activity

The above results strongly predict a dopamine-promoted, $G\alpha_s$- and acetylcholine-dependent, long-term activation of P1 neurons following tap-induced stimulation. Previous studies have also predicted persistent P1 activation but have failed to observe it following a 30-s stimulation protocol (Hoopfer et al., 2015; Inagaki et al., 2014). We delivered 800-ms light pulses to P1 neurons expressing both CsChrimson (Klapoetke et al., 2014) and GCaMP6s (Chen et al., 2013) in naive males that had been isolated from females for 10 days. A single pulse led to a calcium transient that decayed to near baseline over 10–20 s (Figure 8A). When a second light pulse was delivered 1 min later, the calcium signal remained higher above the original baseline and lasted longer (Figure 8A and Video S6). The increase from baseline grew with each additional pulse, while the peak amplitude steadily decreased. Neither the sustained calcium activity, nor the decreasing amplitude was seen in P1 neurons of satiated males (Figure 8B), but both were recovered by bath application of dopamine (Figure 8C), though not if the inter-stimulus interval was expanded to 4 min (Figure 8D). The persistent P1 calcium activity was not rescued in satiated animals by blocking GABA transmission with picrotoxin (Figure 8E), suggesting that dopamine-gated excitatory inputs sustain P1 activity. The nAChR blocker MECA, in contrast, did prevent sustained P1 calcium levels, though not the decrease in

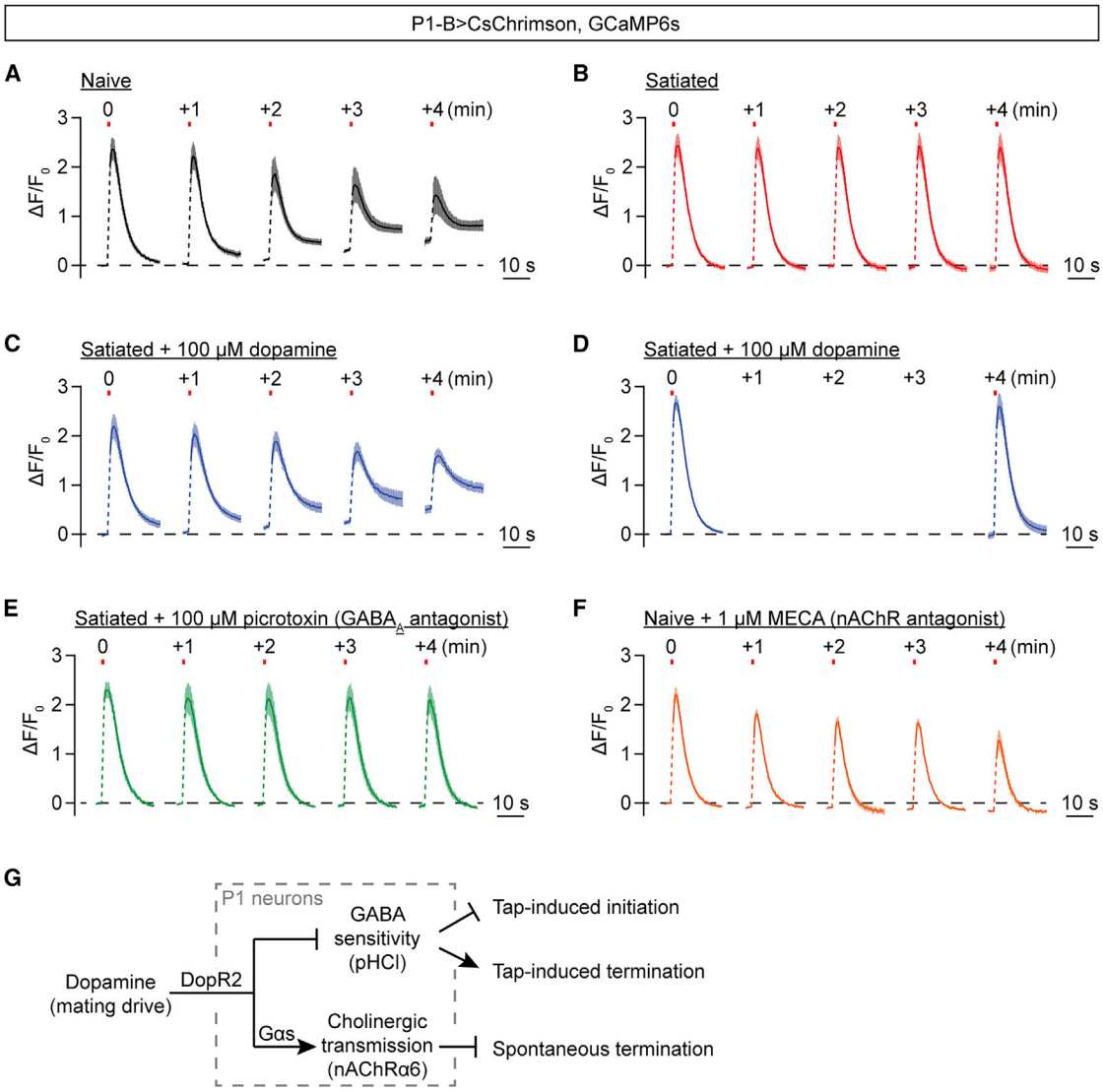

Figure 8. Dopamine Sustains Cholinergic P1 Network Activity for Several Minutes

(A) Spaced 800-ms optogenetic stimulation (once per minute) of P1 neurons reveals graded and persistent calcium transients in brains dissected from 10-day-old males (mean ± SEM, n = 5 brains). See Video S6 for a sample trial.

(B and C) The persistent P1 calcium transients are not seen in brains dissected from satiated 10-day-old males (B) but can be rescued by pre-applying 100 µM dopamine (C) (mean ± SEM, B: n = 4 brains, C: n = 5).

(D) Pre-applying 100 µM dopamine does not induce persistent P1 calcium transients if the inter-pulse interval is increased to 4 min (mean ± SEM, n = 6 brains).

(E) The persistent calcium transients cannot be restored in satiated brains by blocking $GABA_A$ transmission with 100 µM picrotoxin (mean ± SEM, n = 5 brains).

(F) The persistent calcium signal is blocked by pre-applying 1 µM nAChR antagonist MECA (mean ± SEM, n = 6 brains).

(G) Schematic representation of the adjustments dopamine makes to P1 neurons to regulate courtship initiation and termination.

peak amplitude (Figure 8F). Though we cannot formally connect these *ex vivo* effects to the persistent P1 activity required to maintain courtship, the dependence on internal state and specific signaling pathways argue for a shared underlying mechanism: once P1 has been activated, dopamine permits cholinergic excitation onto P1, probably via nAChRα6, to sustain P1 activity. Since dopamine alone does not excite P1 (Figures S4H and S4I), this cholinergic input requires an initial P1 activation, and is therefore recurrent. The level of sustained P1 activity seems to be the product of pre-existing activity and the strength of stimulatory input, which accords well with the more sustained courtship seen from highly motivated males presented with high-quality targets. Through this scalable recurrent excitation, we suggest that dopamine sustains P1 excitation, and the courtship state, for the length of time warranted by the male's reproductive status (Figure 8G).

DISCUSSION

Four hundred years ago, Francis Bacon (d. 1626) wrote: "What chance is in the universe, so will is in man" (Bacon, 1653; quoted

in Durant, 1926). From an outside perspective, motivation can be described as the propensity to engage in a goal-directed behavior under a given set of circumstances. The courtship satiety paradigm allows for repeated trials with a high degree of control over the main variables in decision making: target quality and motivational state. Stabilizing these inputs does not lead to invariant yes-or-no outcomes but instead reveals a fixed probability (Figure 1), likely reflecting the summation of chance neuronal events that initiate with a tap, accrue with signal splitting and propagation, and resolve at P1 excitation. Though sensory input relevant to other behaviors may be more continuous than the brief pulse evoked by a tap, it is often when our attention transiently fixates on an object—perceived or imagined—that we decide to act on it.

What exactly do we mean by chance neuronal events or chance circuit outcomes? John Arbuthnot, in the preface to his translation of Huygens' *Of the Laws of Chance* in 1692, wrote: "It is impossible for a Die, with such determin'd force and direction, not to fall on such determin'd side, only I don't know the force and direction which makes it fall on such determin'd side, and therefore I call it Chance, which is nothing but the want of art" (quoted in Diaconis and Skyrms, 2017). Like the tumbling of a die, there are countless factors that influence the propagation of activity through neural circuits. While these noisy and hidden network variables present problems for sensory and motor systems, we suggest that decision-making circuits may function in a range where chance neuronal events can influence outcomes. By desensitizing a key decision center to inhibition (Figures 2 and 3), motivation essentially weights the die, promoting entry into the behavioral state on a higher fraction of trials. Reliance on chance prevents behavioral inflexibility, allowing a wider range of experiences and the potential for adaptation to new circumstances. The influence of chance on decisions that also integrate perception and motivation makes behavior logical but unpredictable—and therefore interesting.

Once behavior has begun, dopamine-gated recurrent activity reduces (but does not eliminate) the influence of chance, protecting against capricious shifts in behavior before the goal is achieved (Figures 6, 7, and 8). These findings may apply quite broadly, as mammalian feeding, parental, and sleep behaviors are both initiated and sustained by the activity of small subsets of neurons (Betley et al., 2013; Hoopfer et al., 2015; Inagaki et al., 2014; Weber et al., 2015; Wu et al., 2014), and because persistent activity is seen in the mammalian brain (Egorov et al., 2002; Plotkin et al., 2011; Stagkourakis et al., 2018). Dopamine is obligatory in motivating most mammalian behaviors (Palmiter, 2011; Zhou and Palmiter, 1995), so it will be interesting to see whether the mechanisms of desensitization to sensory-evoked inhibition and potentiation of recurrent activity function widely in behavior-specific command neurons to tune the propensities for behavioral selection and persistence. The applicability of these results to mammalian systems may even extend beyond motivation, as dopamine has recently been shown to precede and permit the flow of activity through striatal action-selection circuits (Howe and Dombeck, 2016; da Silva et al., 2018).

Many features of this circuitry remain to be explored in detail. How, for example, does P1 use different GABA receptor complexes to prevent courtship for different reasons (Figure 4)? It may be that different sensory experiences lead to the stimulation of different subsets of mAL neurons. This inhibitory input would then merge with inhibition from volatile pheromones at P1 (Clowney et al., 2015). These categorized inputs might then synapse on separate populations or regions of P1 neurons that express either pHCl or Rdl, which respectively receive motivation-dependent and -independent inhibition. This circuit logic would explain why achieving the necessary threshold of activity is rare if either sensory or drive conditions are violated. But what exactly is this threshold? Since courtship is most often initiated within 500 ms of a tap (Figure 1), the immediate amplitude of activity at P1 likely drives initiation. But how is this amplitude read out? Is there a specific population of neurons that must be sufficiently activated for the system to "catch" and become self-sustaining? While thermogenetic stimulation of P1 neurons dramatically increases courtship probability, it is not immediately sufficient for courtship without a tap (Figure 2). Does that mean that some, or even all, of the thresholding neurons are located outside of P1, or at least are not captured by the P1-B Gal4 line? We know that P1 activity is constantly required during courtship and our data suggest that recurrent excitation sustains the courtship state (Figures 6, 7, and 8). This persistent activity requires a different cholinergic receptor than does initial activation, as well as a specific G protein and prolonged dopaminergic signaling (Figures 7 and S8). Does this again imply neuronal diversity within P1, or are the initiating and sustaining properties shared by all P1 neurons? Also unclear is whether the recurrent loop that sustains P1 activity is confined to P1, or involves other, yet-to-be-discovered neurons. Important mysteries remain downstream of P1 as well, most conspicuously: how does the activity of these ~20 neurons per hemisphere orchestrate the many complex and flexible motor actions that constitute the courtship ritual? In the 10 years since the discovery of P1 (Kimura et al., 2008), a handful of labs have made this circuitry among the best understood in behavioral neuroscience. Given its simplicity, tractability, and the extensive knowledge available in this system, we predict continued and accelerated insights into how behavior is motivated, selected, organized, sustained, and abandoned.

STAR★METHODS

Detailed methods are provided in the online version of this paper and include the following:

- KEY RESOURCES TABLE
- CONTACT FOR REAGENT AND RESOURCE SHARING
- EXPERIMENTAL MODEL AND SUBJECT DETAILS
  - Fly Stocks
- METHOD DETAILS
  - Courtship assays
  - Courtship assays with neuronal activation or silencing
  - Satiating male flies for behavioral and calcium-imaging experiments
  - Two-female choice assays
  - Wide-field calcium and voltage imaging with $P2X_2$ stimulation

SUPPLEMENTAL INFORMATION

Supplemental Information includes eight figures, two tables, and six videos and can be found with this article online at https://doi.org/10.1016/j.neuron.2018.06.014.

ACKNOWLEDGMENTS

We thank Bruce Bean, Mike Do, Jan Drugowitsch, and the members of the Rogulja and Crickmore labs for comments on the manuscript. Jan Drugowitsch pointed us to the compatibility of an evidence-accumulation model with our single-female data. Bernardo Sabatini and Corey Harwell provided help and equipment for two-photon and wide-field microscopy experiments. Ben Gorko helped with the behavioral experiments. The Harvard Neurobiology Imaging Facility provided resources for confocal imaging. Rachel Wilson provided picrotoxin and mecamylamine. The unpublished 13xLexAop-IVS-Syn21-opGCaMP6s (II) and 10xUAS-IVS-Syn21-Chrimson-tdTomato-M19 (II) lines were gifts from Barret Pfeiffer and David Anderson. Adam Claridge-Chang provided the UAS-GtACR1-EYFP stock ahead of publication. S.X.Z. is a Stuart H.Q. & Victoria Quan Fellow at Harvard Medical School. D.R. is a New York Stem Cell Foundation-Robertson Investigator. This work was supported by The New York Stem Cell Foundation.

AUTHOR CONTRIBUTIONS

S.X.Z., L.E.M., and C.L.B. performed the experiments with help from M.A.C. All authors designed the experiments and analyzed data. S.X.Z., D.R., and M.A.C. wrote the manuscript with input from the other authors.

DECLARATION OF INTERESTS

The authors declare no competing interests.

Received: September 29, 2017
Revised: February 19, 2018
Accepted: June 8, 2018
Published: July 5, 2018

REFERENCES

Agrawal, S., Safarik, S., and Dickinson, M. (2014). The relative roles of vision and chemosensation in mate recognition of Drosophila melanogaster. J. Exp. Biol. *217*, 2796–2805.

Anderson, D.J. (2016). Circuit modules linking internal states and social behaviour in flies and mice. Nat. Rev. Neurosci. *17*, 692–704.

Aponte, Y., Atasoy, D., and Sternson, S.M. (2011). AGRP neurons are sufficient to orchestrate feeding behavior rapidly and without training. Nat. Neurosci. *14*, 351–355.

Bacon, F. (1653). De interpretatione naturae sententiae. In The Works of Francis Bacon, pp. 365–370.

Baines, R.A., Uhler, J.P., Thompson, A., Sweeney, S.T., and Bate, M. (2001). Altered electrical properties in Drosophila neurons developing without synaptic transmission. J. Neurosci. *21*, 1523–1531.

Betley, J.N., Cao, Z.F.H., Ritola, K.D., and Sternson, S.M. (2013). Parallel, redundant circuit organization for homeostatic control of feeding behavior. Cell *155*, 1337–1350.

Betley, J.N., Xu, S., Cao, Z.F.H., Gong, R., Magnus, C.J., Yu, Y., and Sternson, S.M. (2015). Neurons for hunger and thirst transmit a negative-valence teaching signal. Nature *521*, 180–185.

Billeter, J.C., Atallah, J., Krupp, J.J., Millar, J.G., and Levine, J.D. (2009). Specialized cells tag sexual and species identity in Drosophila melanogaster. Nature *461*, 987–991.

Boutros, C.L., Miner, L.E., Mazor, O., and Zhang, S.X. (2017). Measuring and altering mating drive in male Drosophila melanogaster. J. Vis. Exp. e55291.

Brown, L.D., Cai, T.T., and DasGupta, A. (2001). Interval estimation for a binomial proportion. Stat. Sci. *16*, 101–133.

Carter, A.G., and Sabatini, B.L. (2004). State-dependent calcium signaling in dendritic spines of striatal medium spiny neurons. Neuron *44*, 483–493.

Chamberland, S., Yang, H.H., Pan, M.M., Evans, S.W., Guan, S., Chavarha, M., Yang, Y., Salesse, C., Wu, H., Wu, J.C., et al. (2017). Fast two-photon imaging of subcellular voltage dynamics in neuronal tissue with genetically encoded indicators. eLife *6*, e25690.

Chen, T.-W., Wardill, T.J., Sun, Y., Pulver, S.R., Renninger, S.L., Baohan, A., Schreiter, E.R., Kerr, R.A., Orger, M.B., Jayaraman, V., et al. (2013). Ultrasensitive fluorescent proteins for imaging neuronal activity. Nature *499*, 295–300.

Chen, Y., Lin, Y.-C., Zimmerman, C.A., Essner, R.A., and Knight, Z.A. (2016). Hunger neurons drive feeding through a sustained, positive reinforcement signal. eLife *5*, e18640.

Clowney, E.J., Iguchi, S., Bussell, J.J., Scheer, E., and Ruta, V. (2015). Multimodal chemosensory circuits controlling male courtship in Drosophila. Neuron *87*, 1036–1049.

da Silva, J.A., Tecuapetla, F., Paixão, V., and Costa, R.M. (2018). Dopamine neuron activity before action initiation gates and invigorates future movements. Nature *554*, 244–248.

Diaconis, P., and Skyrms, B. (2017). Ten Great Ideas about Chance (Princeton University Press).

Drugowitsch, J., Moreno-Bote, R., Churchland, A.K., Shadlen, M.N., and Pouget, A. (2012). The cost of accumulating evidence in perceptual decision making. J. Neurosci. *32*, 3612–3628.

Durant, W. (1926). The Story of Philosophy (Simon and Schuster).

Egorov, A.V., Hamam, B.N., Fransén, E., Hasselmo, M.E., and Alonso, A.A. (2002). Graded persistent activity in entorhinal cortex neurons. Nature *420*, 173–178.

Faisal, A.A., Selen, L.P.J., and Wolpert, D.M. (2008). Noise in the nervous system. Nat. Rev. Neurosci. *9*, 292–303.

Fan, P., Manoli, D.S., Ahmed, O.M., Chen, Y., Agarwal, N., Kwong, S., Cai, A.G., Neitz, J., Renslo, A., Baker, B.S., and Shah, N.M. (2013). Genetic and neural mechanisms that inhibit Drosophila from mating with other species. Cell *154*, 89–102.

Feng, Y., Ueda, A., and Wu, C.-F. (2004). A modified minimal hemolymph-like solution, HL3.1, for physiological recordings at the neuromuscular junctions of normal and mutant Drosophila larvae. J. Neurogenet. *18*, 377–402.

Friggi-Grelin, F., Coulom, H., Meller, M., Gomez, D., Hirsh, J., and Birman, S. (2003). Targeted gene expression in Drosophila dopaminergic cells using regulatory sequences from tyrosine hydroxylase. J. Neurobiol. *54*, 618–627.

Gordon, M.D., and Scott, K. (2009). Motor control in a Drosophila taste circuit. Neuron *61*, 373–384.

Halliday, T. (1983). Motivation. In Animal Behaviour: Causes and Effects, *Volume 1*, T.R. Halliday and P.J.B. Slater, eds. (Blackwell Science), pp. 100–133.

Hoopfer, E.D., Jung, Y., Inagaki, H.K., Rubin, G.M., and Anderson, D.J. (2015). P1 interneurons promote a persistent internal state that enhances inter-male aggression in Drosophila. eLife *4*, e11346.

Howe, M.W., and Dombeck, D.A. (2016). Rapid signalling in distinct dopaminergic axons during locomotion and reward. Nature *535*, 505–510.

Inagaki, H.K., Jung, Y., Hoopfer, E.D., Wong, A.M., Mishra, N., Lin, J.Y., Tsien, R.Y., and Anderson, D.J. (2014). Optogenetic control of Drosophila using a red-shifted channelrhodopsin reveals experience-dependent influences on courtship. Nat. Methods *11*, 325–332.

Kallman, B.R., Kim, H., and Scott, K. (2015). Excitation and inhibition onto central courtship neurons biases Drosophila mate choice. eLife *4*, e11188.

Keleman, K., Vrontou, E., Krüttner, S., Yu, J.Y., Kurtovic-Kozaric, A., and Dickson, B.J. (2012). Dopamine neurons modulate pheromone responses in Drosophila courtship learning. Nature *489*, 145–149.

Kimura, K., Hachiya, T., Koganezawa, M., Tazawa, T., and Yamamoto, D. (2008). Fruitless and doublesex coordinate to generate male-specific neurons that can initiate courtship. Neuron *59*, 759–769.

Klapoetke, N.C., Murata, Y., Kim, S.S., Pulver, S.R., Birdsey-Benson, A., Cho, Y.K., Morimoto, T.K., Chuong, A.S., Carpenter, E.J., Tian, Z., et al. (2014). Independent optical excitation of distinct neural populations. Nat. Methods *11*, 338–346.

Kohatsu, S., and Yamamoto, D. (2015). Visually induced initiation of Drosophila innate courtship-like following pursuit is mediated by central excitatory state. Nat. Commun. *6*, 6457.

Kohatsu, S., Koganezawa, M., and Yamamoto, D. (2011). Female contact activates male-specific interneurons that trigger stereotypic courtship behavior in Drosophila. Neuron *69*, 498–508.

Krashes, M.J., Koda, S., Ye, C., Rogan, S.C., Adams, A.C., Cusher, D.S., Maratos-Flier, E., Roth, B.L., and Lowell, B.B. (2011). Rapid, reversible activation of AgRP neurons drives feeding behavior in mice. J. Clin. Invest. *121*, 1424–1428.

Lima, S.Q., and Miesenböck, G. (2005). Remote control of behavior through genetically targeted photostimulation of neurons. Cell *121*, 141–152.

Liu, Q., Liu, S., Kodama, L., Driscoll, M.R., and Wu, M.N. (2012). Two dopaminergic neurons signal to the dorsal fan-shaped body to promote wakefulness in Drosophila. Curr. Biol. *22*, 2114–2123.

Livneh, Y., Ramesh, R.N., Burgess, C.R., Levandowski, K.M., Madara, J.C., Fenselau, H., Goldey, G.J., Diaz, V.E., Jikomes, N., Resch, J.M., et al. (2017). Homeostatic circuits selectively gate food cue responses in insular cortex. Nature *546*, 611–616.

Manoli, D.S., and Baker, B.S. (2004). Median bundle neurons coordinate behaviours during Drosophila male courtship. Nature *430*, 564–569.

Mohammad, F., Stewart, J.C., Ott, S., Chlebikova, K., Chua, J.Y., Koh, T.-W., Ho, J., and Claridge-Chang, A. (2017). Optogenetic inhibition of behavior with anion channelrhodopsins. Nat. Methods *14*, 271–274.

Mukamel, E.A., Nimmerjahn, A., and Schnitzer, M.J. (2009). Automated analysis of cellular signals from large-scale calcium imaging data. Neuron *63*, 747–760.

Ölveczky, B.P., Andalman, A.S., and Fee, M.S. (2005). Vocal experimentation in the juvenile songbird requires a basal ganglia circuit. PLoS Biol. *3*, e153.

Palmiter, R.D. (2011). Dopamine signaling as a neural correlate of consciousness. Neuroscience *198*, 213–220.

Pan, Y., Meissner, G.W., and Baker, B.S. (2012). Joint control of *Drosophila* male courtship behavior by motion cues and activation of male-specific P1 neurons. Proc. Natl. Acad. Sci. USA *109*, 10065–10070.

Plotkin, J.L., Day, M., and Surmeier, D.J. (2011). Synaptically driven state transitions in distal dendrites of striatal spiny neurons. Nat. Neurosci. *14*, 881–888.

Renart, A., and Machens, C.K. (2014). Variability in neural activity and behavior. Curr. Opin. Neurobiol. *25*, 211–220.

Rendel, J.M. (1945). Genetics and cytology of Drosophila subobscura. II. Normal and selective matings in Drosophila subobscura. J. Genet. *46*, 287–302.

Schnizler, K., Saeger, B., Pfeffer, C., Gerbaulet, A., Ebbinghaus-Kintscher, U., Methfessel, C., Franken, E.M., Raming, K., Wetzel, C.H., Saras, A., et al. (2005). A novel chloride channel in Drosophila melanogaster is inhibited by protons. J. Biol. Chem. *280*, 16254–16262.

Spieth, H.T. (1952). Mating behavior within the genus Drosophila (Diptera). Bull. Am. Mus. Nat. Hist. *99*, 395–474.

Spieth, H.T. (1974). Courtship behavior in Drosophila. Annu. Rev. Entomol. *19*, 385–405.

St-Pierre, F., Marshall, J.D., Yang, Y., Gong, Y., Schnitzer, M.J., and Lin, M.Z. (2014). High-fidelity optical reporting of neuronal electrical activity with an ultrafast fluorescent voltage sensor. Nat. Neurosci. *17*, 884–889.

Stagkourakis, S., Spigolon, G., Williams, P., Protzmann, J., Fisone, G., and Broberger, C. (2018). A neural network for intermale aggression to establish social hierarchy. Nat. Neurosci. *21*, 834–842.

Tervo, D.G.R., Proskurin, M., Manakov, M., Kabra, M., Vollmer, A., Branson, K., and Karpova, A.Y. (2014). Behavioral variability through stochastic choice and its gating by anterior cingulate cortex. Cell *159*, 21–32.

Thistle, R., Cameron, P., Ghorayshi, A., Dennison, L., and Scott, K. (2012). Contact chemoreceptors mediate male-male repulsion and male-female attraction during Drosophila courtship. Cell *149*, 1140–1151.

Toates, F.M. (1986). Motivational Systems. In Problems in the Behavioural Sciences (Cambridge University Press).

Tompkins, L., and Hall, J.C. (1981). The different effects on courtship of volatile compounds from mated and virgin Drosophila females. J. Insect Physiol. *27*, 17–21.

von Philipsborn, A.C., Liu, T., Yu, J.Y., Masser, C., Bidaye, S.S., and Dickson, B.J. (2011). Neuronal control of Drosophila courtship song. Neuron *69*, 509–522.

Weber, F., Chung, S., Beier, K.T., Xu, M., Luo, L., and Dan, Y. (2015). Control of REM sleep by ventral medulla GABAergic neurons. Nature *526*, 435–438.

Wise, R.A., and Rompre, P.P. (1989). Brain dopamine and reward. Annu. Rev. Psychol. *40*, 191–225.

Wu, Z., Autry, A.E., Bergan, J.F., Watabe-Uchida, M., and Dulac, C.G. (2014). Galanin neurons in the medial preoptic area govern parental behaviour. Nature *509*, 325–330.

Yamamoto, D., and Koganezawa, M. (2013). Genes and circuits of courtship behaviour in Drosophila males. Nat. Rev. Neurosci. *14*, 681–692.

Yao, Z., Macara, A.M., Lelito, K.R., Minosyan, T.Y., and Shafer, O.T. (2012). Analysis of functional neuronal connectivity in the Drosophila brain. J. Neurophysiol. *108*, 684–696.

Zhang, S.X., Rogulja, D., and Crickmore, M.A. (2016). Dopaminergic circuitry underlying mating drive. Neuron *91*, 168–181.

Zhou, Q.Y., and Palmiter, R.D. (1995). Dopamine-deficient mice are severely hypoactive, adipsic, and aphagic. Cell *83*, 1197–1209.

STAR★METHODS

KEY RESOURCES TABLE

REAGENT or RESOURCE	SOURCE	IDENTIFIER
Antibodies		
Mouse anti-GFP clone 3E6	Thermo Fisher Scientific	A-11120, AB_221568
Alexa Fluor 488 donkey anti-mouse	Thermo Fisher Scientific	A-21202, AB_141607
Chemicals, Peptides, and Recombinant Proteins		
All-trans-retinal	Sigma-Aldrich	R2500
Picrotoxin	Sigma-Aldrich	P1675
Mecamylamine	Sigma-Aldrich	M9020
Dopamine	Alfa Aesar	A11136-06
ATP disodium salt hydrate	Sigma-Aldrich	A2383
Experimental Models: Organisms/Strains		
D. melanogaster: w^{1118}/Dp(2;Y), P{hs-hid}Y	Bloomington Drosophila Stock Center (BDSC)	BDSC: 24638
D. m.: wild-type Canton S	Keleman et al., 2012	Flybase: FBsn0000274
D. m.: w*; P{UAS-TrpA1(B).K}attP16	BDSC	BDSC: 26263
D. m.: w^{1118};; P{ple-GAL4.F}3	Friggi-Grelin et al., 2003	Flybase: FBti0072936
D. m.: w^{1118};; P{VT002857-Gal4}attP2	Vienna Drosophila Resource Center (VDRC)	VDRC: 200494
D. m.: y*, w*;; P{w[+mW.hs] = GawB}mura[NP5945]/TM6, P{w[-] = UAS-lacZ.UW23-1}UW23-1	Kyoto Drosophila Genomics and Genetic Resources	DGGR: 105062
D. m.: DopR2-RNAi: w^{1118}; P{KK110947}VIE-260B	VDRC	VDRC: 105324
D. m.: P1-B-Gal4: w^{1118};; P{GMR71G01-GAL4}attP2	BDSC	BDSC: 39599
D. m.: w^{1118}; P{w[+mC] = UAS-Dcr-2.D}2	BDSC	BDSC: 24650
D. m.: w^{1118};; P{w[+mC] = UAS-Dcr-2.D}10	BDSC	BDSC: 24651
D. m.: w^{1118}; P{UAS-eGFP-Kir2.1}/CyO	Baines et al., 2001	Flybase: FBtp0110871
D. m.: w*;; P{tubP-GAL80ts}2/TM2	BDSC	BDSC: 7017
D. m.: $AbdB^{LDN}$-Gal4: y^1, w*;; P{GawB}Abd-BLDN/TM6B, Tb^1	BDSC	BDSC: 55848
D. m.: mAL-S-Gal4: w^{1118};; P{GMR43D01-GAL4}attP2	BDSC	BDSC: 64345
D. m.: mAL-R-LexA: w^{1118}; P{GMR25E04-lexA}attP40	BDSC	BDSC: 61524
D. m.: w^{1118}; P{LexAop-IVS-Syn21-opGCaMP6s}su(Hw)attP5	Gift from B.D. Pfeiffer and D.J. Anderson	N/A
D. m.: w^{1118}; P{10xUAS-IVS-Syn21-Chrimson-tdTomato-M19}su(Hw)attP5	Gift from B.D. Pfeiffer and D.J. Anderson	N/A
D. m.: w^{1118};; P{UAS-Rnor＼P2rx2.L}	Lima and Miesenböck, 2005	Flybase: FBtp0021869
D. m.: P1-B-LexA: w^{1118}; P{GMR71G01-LexA}attP40	BDSC	BDSC: 54733
D. m.: w^{1118};; P{lexAop-P2X2.Y}	Yao et al., 2012	Flybase: FBtp0093385
D. m.: w^{1118}; P{UAS-IVS-GCaMP6s}attP40	BDSC	BDSC: 42746
D. m.: w^{1118}; P{UAS-ASAP1}attP40	BDSC	BDSC: 65412
D. m.: w^{1118}; PBac{UAS-ASAP2s}VK00005	BDSC	BDSC: 76247
D. m.: y^1, w*; PinYt/CyO; P{UAS-mCD8::GFP.L}LL6	BDSC	BDSC: 5130
D. m.: Rdl-RNAi-1: w^{1118}; P{KK104293}VIE-260B	VDRC	VDRC: 100429
D. m.: Rdl-RNAi-2: y^1, v^1;; P{TRiP.JF01227}attP2	BDSC	BDSC: 31286
D. m.: pHCl-RNAi: w^{1118}; P{KK112646}VIE-260B	VDRC	VDRC: 103247
D. m.: +;; $DopR2^{attP}$	Keleman et al., 2012	N/A
D. m.: Gαs-RNAi-1: y1 v1;; P{TRiP.HMC03106}attP2	BDSC	BDSC: 50704

(*Continued on next page*)

Continued

REAGENT or RESOURCE	SOURCE	IDENTIFIER
D. m.: Gαs-RNAi-2: y1 v1;; P{TRiP.JF03255}attP2	BDSC	BDSC: 29576
D. m.: nAChRα3-RNAi-1: y1 v1; P{TRiP.HMJ23004}attP40/CyO	BDSC	BDSC: 61225
D. m.: nAChRα3-RNAi-2: y^1, v^1;; P{TRiP.JF03255}attP2	BDSC	BDSC: 27671
D. m.: nAChRα6-RNAi-1: y^1, sc*, v^1; P{TRiP.HMC03623}attP40	BDSC	BDSC: 52885
D. m.: nAChRα6-RNAi-2: y^1, v^1; P{TRiP.HMJ21826}attP40/CyO	BDSC	BDSC: 57818
D. m.: w^{1118};; P{20xUAS-IVS-Syn21-CsChrimson-tdTomato}attP2	Hoopfer et al., 2015	N/A
D. m.: w^{1118};; P{ple-GAL4.TH-C'}/Sb	Liu et al., 2012	Flybase: FBtp0083572
D. m.: w^{1118}; P{ple-GAL4.TH-D'}/CyO	Liu et al., 2012	Flybase: FBtp0083573
D. m.: w^{1118};; P{ple-GAL4.TH-F}1/Sb	Liu et al., 2012	Flybase: FBti0151785
D. m.: w^{1118};; P{ple-GAL4.TH-G}1/Sb	Liu et al., 2012	Flybase: FBti0151784
D. m.: PPN1-S-Gal4: w^{1118};; P{GMR56C09-GAL4}attP2	BDSC	BDSC: 39145
D. m.: w^{1118}; P{LexAop-CD8::spGFP11}; P{UAS-CD4-spGFP1-10}	Gordon and Scott, 2009	N/A
D. m.: w^{1118};; P{UAS-IVS-GtACR1}attP2	Mohammad et al., 2017	N/A
Software and Algorithms		
2-photon calcium-imaging analysis package (MATLAB)	Zhang et al., 2016	https://github.com/CrickmoreRoguljaLabs/Ca2plus
ROI-based fluorescence quantification package (MATLAB)	Zhang et al., 2016	https://github.com/CrickmoreRoguljaLabs/Blind-image-analysis
Courtship-initiation analysis package (MATLAB)	This paper	https://github.com/CrickmoreRoguljaLabs/tapping-codes
Simulation package for linear evidence accumulation (MATLAB)	This paper	https://github.com/CrickmoreRoguljaLabs/Tap_EvidenceAccumulation
Jeffrey's 95% confidence interval (MATLAB)	This paper	https://github.com/CrickmoreRoguljaLabs/Jeffi
Two-sample Kolmogorov-Smirnov test (MATLAB)	This paper	https://github.com/CrickmoreRoguljaLabs/KSstat
Other		
Phosphate Buffered Saline 10x	MediaTech	46-013-CM
Triton X-100	Sigma-Aldrich	X100
Potato flakes	Carolina Biological Supply	173200
Nunc Petri Dishes	Thermo Scientific	150318
655-nm LED	Luxeon Star LEDs	LXM3-PD01-0350
530-nm LED	Luxeon Star LEDs	LXML-PM01-0100
Arduino MEGA	Arduino	A000067
Raspberry PI Model B+	Raspberry PI	Model B+

CONTACT FOR REAGENT AND RESOURCE SHARING

Please contact Dragana Rogulja (Dragana_Rogulja@hms.harvard.edu) or the Lead Contact Michael A. Crickmore (Michael.Crickmore@childrens.harvard.edu) for fly strains and other resources in this study.

EXPERIMENTAL MODEL AND SUBJECT DETAILS

Fly Stocks

Fly husbandry was performed as previously described (Zhang et al., 2016). Flies were maintained on conventional cornmeal-agar medium under a 12-hour light/12-hour dark cycle at 25°C and ambient humidity. Due to the focus of this study, all tested flies were adult males. Unless otherwise stated, males were collected on the day of eclosion and group-housed away from females for 3-4 days before testing. Virgin females were generated by heat-shocking a w^{1118} stock with a hs-hid transgene integrated on the Y chromosome (Bloomington stock #24638) in a 37°C water bath for 60 minutes. All behavioral experiments were carried out between ZT 1 and ZT 10 (lights are turned ON at ZT 0 and turned OFF at ZT 12). Detailed genotypes of all strains used in the paper are listed in Table S2 available online.

METHOD DETAILS

Courtship assays

Courtship assays were carried out in the same setting as previously described (Boutros et al., 2017; Zhang et al., 2016). A male fly (3-4 days old) and a w^{1118} virgin female fly were videotaped in cylindrical courtship chambers (10 mm diameter and 3 mm height) at 23°C and ambient humidity. We noticed that taps occur more frequently in smaller chambers, so it is possible that these chambers might lead to an increased reliance on tapping (and under-reliance on other sensory modalities) than would be seen in more naturalistic circumstances. For male-male courtship assays, w^{1118} males were used as courtship targets instead.

Courtship assays with neuronal activation or silencing

Assays were generally performed as described above. For thermogenetic experiments using TrpA1, half of the males were assayed at 23°C, while the other half were pre-incubated at a higher temperature (28.5°C or 30°C) for 5 minutes before being introduced to females and assayed at the same temperature (28.5°C or 30°C). For conditional silencing experiments involving $TubGal80^{ts}$, male flies were moved to 30°C after eclosion and kept there (isolated from females) until just before the assay, which took place at 23°C. For optogenetic experiments using CsChrimson, Chrimson-M19, and GtACR1, newly eclosed male flies were transferred to aluminum-foil-wrapped vials containing rehydrated potato flakes and 100 μL of all-trans-retinal stock solution (50 mM in ethanol) for 3 days. In the case of GtACR1 experiments, which also use $TubGal80^{ts}$, male flies were kept at 30°C for 3 days before experiments.

In CsChrimson experiments (Figure 6H), males were assayed under ambient light conditions until a brief 1 s pulse of 655-nm red light (~100 $\mu W/mm^2$) was delivered during courtship. In GtACR experiments (Figure 6I), males were assayed under ambient light conditions until a brief 1 s or 5 s pulse of 530-nm green light (~5 $\mu W/mm^2$) was delivered during courtship. In Chrimson-M19 experiments (Figure 7A), pre-satiated males were assayed under ambient light (Figure 7A, left), under 655-nm red light (~100 $\mu W/mm^2$) (Figure 7A, middle), or pre-stimulated under the same light for 5 minutes before paired with females (light is still on) (Figure 7A, right).

Satiating male flies for behavioral and calcium-imaging experiments

To satiate them before a courtship assay, males were individually paired with 15-20 virgin w^{1118} females in food vials at 23°C for 1 hour (in experiments using Kir2.1 or RNAi) or, by default, for 4.5 hours (in experiments using TrpA1) before aspirating the male into a standard courtship assay. The same procedure was used for calcium imaging experiments. For CsChrimson-expressing males, the satiety assays were carried out in vials floored with retinal-containing food. These vials were mostly wrapped with aluminum foil except for a ~2 mm gap on the top to provide some light to assist courtship. Male flies in this condition were able to be satiated (our observations).

Two-female choice assays

In Figure 5, the courtship assays involved a male fly with two females, one virgin and the other mated. To differentiate between the two females when scoring the assays, we used females of different eye colors, but the correspondence between eye colors and mating states were randomized for each trial and blinded to the experimenter. In each trial, the male fly was allowed to tap the females up to 10 times, and the courtship choice was scored when the male displays any courtship step (see below) toward either female.

Wide-field calcium and voltage imaging with $P2X_2$ stimulation

An upright Leica DM5500 B scope was used for calcium imaging experiments involving $P2X_2$ stimulation. Brains of 3-day old male flies expressing GCaMP6s and $P2X_2$ were dissected out and mounted, posterior side down, onto the center of a coated Petri dish containing 3 mL of HL3.1 saline solution (Feng et al., 2004). This preparation preserves P1 and mAL neurons, but severs the afferent projections of vAB3 neurons. GCaMP6s fluorescence of the lateral-protocerebrum projection of P1 or mAL neurons were identified with baseline GCAMP6s fluorescence and imaged for 150 frames at a rate of 1 frame/second. At Frame #40, 20 μL 150 mM ATP solution (pH pre-adjusted) was carefully pipetted along the inside edge of the Petri dish to reach a final concentration of 1 mM. For 4-5 experiments of each condition, the imaging sessions were extended to 250 frames, and 20 μL 3M KCl solution (pH pre-adjusted) was added at Frame #140 to test if the neurons were alive. These data are shown in Figures S5C and S5D.

ASAP experiments follow the same protocol. Since mAL-S-LexA (R43D01) was not available when we performed the experiments, we used mAL-R-LexA (R25E04, named after the Ruta lab where it was first characterized), to drive $P2X_2$.

Two-photon calcium imaging with CsChrimson stimulation

Two-photon laser-scanning microscopy was performed using a custom microscope as previously described (Carter and Sabatini, 2004). Most of the procedures are the same as in (Zhang et al., 2016). Newly eclosed flies were transferred to coated vials containing rehydrated potato flakes and 100 μL of 50 mM all-trans-retinal. Brains of 10-day old male flies expressing CsChrimson and GCaMP6s in P1-B neurons were dissected under low-light conditions and mounted, posterior side down, onto a coated Petri dish as in the $P2X_2$ stimulation experiments. The lateral protocerebrum projection of P1 neurons was identified with baseline GCaMP6s fluorescence excited at 820 nm (the isosbestic point of GCaMP). Note that this region likely contains projections from multiple P1 neurons. GCaMP6s was excited at 910 nm and 11.8 mW at the sample, and light was collected in 128x128 frames at 256 ms per frame.

The laser power was kept consistent and minimal to avoid any 2-photon activation of CsChrimson. At Frame #24, an 800-ms long pulse of red light (655 nm) was delivered using an LED (see Zhang et al., 2016 for descriptions), during which no fluorescence data were collected to protect the photomultiplier tube.

Assaying neuronal connectivity with GRASP

GRASP experiments labeling connections between mAL and P1-B neurons were performed as described before (Zhang et al., 2016). Briefly, fly brains were dissected in Schneider's medium and immediately fixed in 4% paraformaldehyde dissolved in PBS with 0.3% Triton X-100 (PBST) for 20 minutes. After 3x 20-minute washes with PBST, the brains were incubated with the primary antibody against GFP (1:2000 diluted in PBST) at 4°C for 48 hours. After another round of 3x 20-minute washes with PBST, the brains were incubated with the secondary antibody (1:400 diluted in PBST) at 4°C for 48 hours. Then, after a final round of 3x 20-minute washes, the brains were mounted on a glass slide using standard procedures. Confocal sections were acquired using an Olympus Fluoview 1000 microscope at 3-μm intervals.

Pharmacology

Dopamine was prepared in a 100 mM stock solution in ddH_2O. Picrotoxin (PTX) was prepared as a 5 mM stock solution in 150 mM NaCl. Mecamylamine (MECA) was prepared in a 1 mM stock solution in ddH_2O. For all experiments, dopamine (100 μM), picrotoxin (100 μM), or MECA (1 μM) were applied 10 minutes before ATP or optogenetic stimulation.

QUANTIFICATION AND STATISTICAL ANALYSIS

Analysis of courtship and tapping behaviors

After one of us (L.E.M. or C.L.B.) took the videos, a different experimenter (S.X.Z.) scored courtship initiations and terminations, blind to genotypes and experimental conditions. The courtship index was manually scored as the fraction of time during which the male fly is engaged in mating behaviors (courtship and copulation) within 5 minutes after courtship initiation. For analysis of courtship initiation, we scored tapping as a male foreleg touching any part of the female body. A bout of courtship was scored as initiated when the male oriented toward the female, began tracking her, and unilaterally extended his wing to sing to her. In Figure 6A, the average bout lengths were calculated using only bouts that did not lead to copulation. A bout was scored as terminated if the male stopped tracking or turned away from the female. Once courtship is terminated, it is almost never reinitiated within 10 s. Whenever possible, terminations were also verified by the male not resuming courtship without tapping when the female passed in front of him again. A termination is classified as tap-induced if it occurred within 1 s following the male foreleg contacting the female body (also referred to as a tap). Otherwise, it is classified as spontaneous. If the male fly did not court within the first 15 minutes of each assay, the courtship index was scored as 0. Courtship latency was scored as the delay preceding the first courtship initiation after the male fly was paired with the female.

Linearizing cumulative courtship initiation curve

Cumulative courtship initiation percentages were linearized according to a coin-flip model in which the odds of courtship initiation do not change from tap to tap. Therefore, if each tap has a p probability of initiating courtship, the cumulative probability of courtship initiation y after x taps is expressed as [1 - probability of not initiating courtship], which is $[1 - (1 - p)^x]$. The equation $y = [1 - (1 - p)^x]$ can be linearized to $Ln(1 - y) = Ln(1 - p) * x$. For more intuitive visualization, we inverted the signs on both sides and used the equation $-Ln(1 - y) = -Ln(1 - p) * x$ instead. For each experiment, we first obtained the cumulative courtship initiation percentages $[y_1, y_2, y_3, y_4]$ after taps [1, 2, 3, 4]. Then, we plotted the linearized y values $[-Ln(1 - y_1), -Ln(1 - y_2), -Ln(1 - y_3), -Ln(1 - y_4)]$ against the x values [1, 2, 3, 4], and fitted the graph with a line that is forced through the point of origin [0, 0]. Since the slope of the line equates $-Ln(1 - p)$, we can obtain the courtship probability p from the slope. If all flies initiate courtship after a certain number (X_{all}) of taps (e.g., Figure 2B), data points before X_{all} were used instead. Finally, for the figures, we used a 0-to-98% scale (0-to-3.912 after linearization) for the y-axes, marked with 30%, 60%, and 90% ticks (0.357, 0.916, and 2.303 respectively after linearization). See the section below for generating 95% confidence intervals of courtship probabilities. The MATLAB programs to perform these calculations are available online.

Generating R^2 distributions

To generate R^2 distributions, we used either permutation (Figures S1B and S1C) or simulated coin flips (Figure S1D) to generate courtship initiation data of n flies. As an example of permutation, we used n = 55 flies in Figure S1B to match the naive-fly experiment in Figure 1C, and generated 455,126 unique possibilities: [0, 0, 0, 0], [0, 0, 0, 1], [0, 0, 0, 2], [0, 0, 0, 3] … [55, 55, 55, 55]. To simulate coin flips for an experiment (e.g., WT naive males in Figure 1E), we used the matching coin number (number of flies, e.g., n = 55) and coin odds (courtship probability, e.g., 44%) in each iteration to generate 100,000 combinations of data: [21, 37, 46, 49], [26, 36, 45, 53], etc. We then performed the linearization and linear regression (described above) on all the possibilities, generating an R^2 value for each possibility. In the example shown in Figure S1B, the R^2 values range from -345 to ~ 1 (only the values between 0 and 1 are shown for clarity) with 365 R^2 values equal or above our experimental result of 0.995, giving a p value < 0.001.

In Figures S1C and S1D, we generated a p value for each R^2 value in all 109 linear regressions of courtship initiations (see Table S1) in this paper, using R^2 distributions from either permutations (Figure S1C) or simulated coin flips (Figure S1D). We then plotted the cumulative distribution function of the p values. A diagonal line is used to show the theoretical p value distribution if our empirical data were generated purely from permutations (Figure S1C) or coin flips (Figure S1D).

Generating 95% confidence intervals in estimating courtship probabilities

For each linear regression (see Table S1 for a list), 100,000 iterations of bootstrapping were used to generate the 95% confidence intervals of courtship probabilities. In each iteration, we constructed a bootstrapped dataset of the same size by randomly resampling, with replacement, from the experimental data. Then we performed the same linearization and linear regression as described above to obtain a bootstrapped courtship probability. All bootstrapped courtship probabilities were ranked, and then the cutoff points for the highest/lowest 2.5% were marked as the 95% confidence interval (Table S1). The MATLAB program to perform these calculations is available online.

Hypothesis testing for courtship probabilities

Bootstrapping was used to calculate the p values between pairs of courtship probabilities (e.g., Dataset X and Dataset Y), with the underlying null hypothesis that these two datasets were generated with the same unknown courtship probability. Before bootstrapping, we pooled the datasets X and Y together to generate a new dataset P, whose size is the sum of that of X (N_X) and Y (N_Y). In each iteration, we first randomly resampled, with replacement, two bootstrapped datasets B_X and B_Y from the pooled dataset. Then, using the same linearization and linear regression procedures above, we calculated the bootstrapped courtship probabilities from these two new datasets (CP_{BX} and CP_{BY}). Last, we calculated the absolute difference between these two courtship probabilities ($|CP_{BX} - CP_{BY}|$) and repeated this process for 100,000 iterations. The p value was calculated as the fraction of all iterations in which the differences in bootstrapped courtship probabilities ($|CP_{BX} - CP_{BY}|$) were at least as large as the difference in experimentally determined courtship probabilities ($|CP_X - CP_Y|$). In cases of multiple comparisons (e.g., Figure 1E), we used Bonferroni corrections to adjust the p values accordingly. The MATLAB program to perform these calculations is available online.

Evidence-accumulation simulation for courtship initiation

We used an evidence accumulation model that samples from Gaussian-distributed evidence pools. This distribution is set to have a standard deviation of 1 as well as a mean value that depends on male's satiety state and target quality (e.g., mean = 0.8 for courtship by naive males toward virgin females). Then, for each simulated male, each tap randomly samples an evidence value from the distribution, and the evidence value is accumulated without loss between taps. Once evidence is accumulated past a threshold value (set to 1) after X taps, the male is marked as starting courtship after X taps. In Figure S6, we performed 100,000 iterations of simulations for each mean evidence value ranging from −0.5 to 1.5 and analyzed the courtship initiation percentages the same way as we did with experimental data (e.g., Figure 1E). The MATLAB program to perform these calculations is available online.

Simulation and analysis of a two-female choice assay

In Figure 5, we performed 103 trials of choice assays, in which a male chooses from a virgin female and a mated female. For comparison, we also performed simulations of the same experiment (100,000 iterations of 103 males each), assuming the male exclusively uses the coin-flip model (Coin-flipper) or the evidence accumulation model (Accumulator). In both the experiment and the simulation, the male fly is allowed to freely tap both females for up to a total of 10 taps. Since we could not pre-determine the fractions of taps on the virgin and the mated females, we performed the simulations for a range of tapping fractions. To simulate Coin-flippers, we use 45% and 7% per-tap probability for initiating courtship toward virgin and mated females respectively (based on data in Figure S1F). To simulate Accumulators, we use 0.8 and −0.4 mean evidence for initiating courtship toward virgin and mated females respectively (based on results in Figure S6M).

From both experimental data and simulation results, we calculated the percentages of courtship initiations toward the virgin females (Figure 5B), courtship initiations toward mated females (Figure 5C), and courtship initiations toward all females (Figure 5D). We use F_1 score to quantify the preference of virgin females over mated ones, using the formula F_1 = 2 x Precision x Recall / (Precision + Recall). Precision is defined as [Courtship initiations toward virgin females] / [Total courtship initiations], and Recall is defined as [Courtship initiations toward virgin females] / [Total taps on virgin females]. F_1 scores range from 1 (perfectly selective to virgin females) to 0 (perfectly selective to mated females). In Figure 5E, we also estimate the Mean ± 95% C.I. F_1 score of a male that cannot tell the difference between virgin and mated females (by shuffling experimental data). The MATLAB programs to perform these calculations are available online.

Generating chance levels of tap-induced termination

In Figure 6D, chance levels of tap-induced termination were calculated using the equation ([Tap-induced termination count] + [Spontaneous termination count]) / [courtship time] * [Tapping frequency during courtship] * [1 s window].

Quantifying imaging data

For wide-field imaging, fluorescence data were analyzed by selecting a region of interest from a pre-stimulation frame of the lateral protocerebrum. The regions of interest were kept roughly the same size between experiments. GCamp6s data are presented as $\Delta F/F_0$. ASAP1 or ASAP2s data are presented as $-\Delta F/F_0$ to correct the inverse relation between sensor fluorescence and membrane voltage. Hypothesis testing was done with either a t test or a one-way ANOVA of max $\Delta F/F_0$ (min $-\Delta F/F_0$ in the case of voltage imaging).

For 2-photon imaging experiments, fluorescence data were analyzed in MATLAB using a semi-automated program modified from a published independent component analysis algorithm (Mukamel et al., 2009). The program is available online. Data are presented as $\Delta F/F_0$.

For GRASP experiments, after one person (S.X.Z.) took the images, another person (L.E.M.-blind to satiety states) selected regions of interest (ROIs) and background. ROI sizes were kept roughly the same between samples. Average pixel fluorescence in each ROI was calculated with a custom-written program in MATLAB (Mathworks). The program is available online.

Additional statistical tests

One-way ANOVA (with Tukey post hoc correction) and Fisher's exact test were performed using Prism 7. The 95% confidence intervals (C.I.) of termination frequencies were calculated using Jeffrey's prior (Brown et al., 2001) in MATLAB. The 95% C.I. of courtship probabilities and the statistical significance of the differences between courtship probabilities were calculated with bootstrapping (see above). Kolmogorov–Smirnov test (Figures S1C and S1D) was calculated in MATLAB. The programs are available online.

DATA AND SOFTWARE AVAILABILITY

All MATLAB programs used in this study are available online.

1) The MATLAB package to quantify 2-photon calcium imaging data is available at https://github.com/CrickmoreRoguljaLabs/Ca2plus.
2) The MATLAB package to quantify GRASP signals is available at https://github.com/CrickmoreRoguljaLabs/Blind-image-analysis.
3) The MATLAB package to linearize courtship initiations (CPline), simulate coin flips (coinsim_batch), permutate courtship initiations (TapPermute), calculate the 95% confidence intervals of courtship probabilities (TapCI), and perform hypothesis testing on pairs of courtship probabilities (TapHyp) is available at https://github.com/CrickmoreRoguljaLabs/tapping-codes.
4) The MATLAB package to simulate evidence accumulation between taps and simulate the performance of males in two-female choice assays is available at https://github.com/CrickmoreRoguljaLabs/Tap_EvidenceAccumulation.
5) The MATLAB function to calculate Jeffrey's 95% confidence interval is available at https://github.com/CrickmoreRoguljaLabs/Jeffi.
6) The MATLAB function to perform two-sample Kolmogorov-Smirnov tests is available at https://github.com/CrickmoreRoguljaLabs/KSstat.